



저작자표시-비영리-변경금지 2.0 대한민국

이용자는 아래의 조건을 따르는 경우에 한하여 자유롭게

- 이 저작물을 복제, 배포, 전송, 전시, 공연 및 방송할 수 있습니다.

다음과 같은 조건을 따라야 합니다:



저작자표시. 귀하는 원저작자를 표시하여야 합니다.



비영리. 귀하는 이 저작물을 영리 목적으로 이용할 수 없습니다.



변경금지. 귀하는 이 저작물을 개작, 변형 또는 가공할 수 없습니다.

- 귀하는, 이 저작물의 재이용이나 배포의 경우, 이 저작물에 적용된 이용허락조건을 명확하게 나타내어야 합니다.
- 저작권자로부터 별도의 허가를 받으면 이러한 조건들은 적용되지 않습니다.

저작권법에 따른 이용자의 권리는 위의 내용에 의하여 영향을 받지 않습니다.

이것은 [이용허락규약\(Legal Code\)](#)을 이해하기 쉽게 요약한 것입니다.

[Disclaimer](#)

Master's Thesis

석사학위논문

All Joints Controlling Master Device for Y-Type  
Single Port Laparoscopic Surgery Robot

Seongbo Shim(심 성 보 沈 晟 輔)

Department of Robotics Engineering

로봇공학전공

**DGIST**

**2015**

Master's Thesis

석사학위논문

# All Joints Controlling Master Device for Y-Type Single Port Laparoscopic Surgery Robot

Seongbo Shim (심 성 보 沈 晟 輔)

Department of Robotics Engineering

로봇공학전공

**DGIST**

**2015**

# All Joints Controlling Master Device for Y-Type Single Port Laparoscopic Surgery Robot

Advisor : Professor Jaesung Hong

Co-advisor : Professor Taehun Kang

by

Name

Department of Robotics Engineering  
DGIST

A thesis submitted to the faculty of DGIST in partial fulfillment of the requirements for the degree of Master of Science. The study was conducted in accordance with Code of Research Ethics<sup>1</sup>

. .2015

Approved by

Professor Jaesung Hong (\_\_\_\_\_)  
(Advisor)

Professor Taehun Kang (\_\_\_\_\_)  
(Co-Advisor)

---

<sup>1</sup> Declaration of Ethical Conduct in Research: I, as a graduate student of DGIST, hereby declare that I have not committed any acts that may damage the credibility of my research. These include, but are not limited to: falsification, thesis written by someone else, distortion of research findings or plagiarism. I affirm that my thesis contains honest conclusions based on my own careful research under the guidance of my thesis advisor.

# All Joints Controlling Master Device for Y-Type Single Port Laparoscopic Surgery Robot

Seongbo Shim

Accepted in partial fulfillment of the requirements for the degree of Master of  
Science.

. .2015

Head of Committee	Professor Jaesung Hong	(인)
Committee Member	Professor Taehun Kang	(인)
Committee Member	Professor Pyunghun Chang	(인)

MS/RT  
201323006

심 성 보. Seongbo Shim. The study of a master device to control all joints of Y-type single port surgery robot. Department of robotics Engineering. 2015. 52p.  
Advisors Prof. Jaesung Hong, Co-Advisors Prof. Taehun Kang

### ABSTRACT

Recently, a number of Y-type robot for single port laparoscopic surgery (SPLS) have been developed. Considering that all joints of the robot are inserted in the human body during the surgery, the general master device which controls the only tip of the robot is not suitable. The reason is that some joint operation will not be under control and may damage tissues in the tip controlling method. In this paper, we propose an ergonomic master device for Y-type SPLS robot to control all joints separately. The designed master device has two main features: (1) In order to reduce fatigue of operators during the surgery, ergonomic design and counterbalanced mechanism are applied to the master device. (2) To minimize the velocity error of tips between master and slave, the mapping factors of each joint are calculated and implemented. Consequently, we have designed all joints controlling master device ergonomically, and found the mapping factors to have minimum a velocity error of both tips. We verified that operators can manipulate the slave robot intuitively and both tips have similar velocity through the simulation.

Keywords: Single port surgery robot, Master device, All joints control, Ergonomic design

# Contents

Abstract .....	i
List of contents .....	iii
List of tables .....	vi
List of figures .....	vii

# List of contents

I. INTRODUCTION .....	1
1.1 Introduction to Single Port Laparoscopic Surgery (SPLS).....	1
1.2 Previous researches of robotic SPLS.....	3
1.3 Previous researches of master device .....	6
1.4 Design factors of master device .....	8
1.5 Research contents and goals.....	10
II. DESIGN CONSIDERATION OF MASTER DEIVCE .....	12
2.1 Slave robot for single port laparoscopic surgery .....	12
2.2 Ergonomic .....	15
2.1.1 Joints arrangement .....	16
2.1.2 Balance of the positioning stage .....	19
2.3 Sensors and material.....	23
III. KINEMATICS ANALYSIS AND MAPPING FACTORS .....	24
3.1 Forward kinematics .....	27
3.2 Inverse kinematics.....	28
3.3 Jacobian analysis .....	30
3.4 Mapping factors.....	33
IV. EXPERIMENTS AND RESULTS.....	41
4.1 Mesurging velocity and results.....	41
4.2 Simulation with virtual slave robot and result.....	44
V. DISCUSSION AND CONCLUSIONS.....	46

## List of tables

Table 1. D-H parameters of PLAS .....	14
Table 2. D-H parameters of the first master device .....	16
Table 3. D-H parameters of the designed master device .....	25
Table 4. D-H parameters of the reconstructed slave robot.....	35
Table 5. D-H parameters of the reconstructed master device.....	37
Table 6. Mapping factors between master and slave .....	39

## List of figures

Figure 1. Development of surgical techniques and operation wounds.....	2
Figure 2. Master-Slave system for da Vinci SI.....	4
Figure 3. X-type and Y-type robot for SPLS.....	5
Figure 4. X-type slave robot (da Vinci SI system) and Y-type slave robot (PLAS) .....	5
Figure 5. Tip controlling master device (da Vinci) and all joints controlling master device (TELESAR II).....	7
Figure 6. Type of robotic SPLS platform; X-type (left), Y-type (middle), PLAS (right) .....	13
Figure 7. (A) CAD model and (B) prototype of PLAS.....	13
Figure 8. Kinematic representation of PLAS .....	14
Figure 9. (A) CAD and (B) kinematic model of the first master device for Y-type SPLS robot.....	17
Figure 10. CAD model of the second master device for Y-type SPLS robot .....	18
Figure 11. Prototype of the second master device for Y-type SPLS robot.....	19
Figure 12. Angle of joint 4 without conterbalancing .....	20
Figure 13. A simple schematic darwing of stagin position .....	20
Figure 14. A simple schematic darwing of stagin position about joint 4 .....	21
Figure 15. Angle of joint 4 with conterbalancing .....	22
Figure 16. Kinematic representation of the designed master device .....	25
Figure 17. Start and end joint of the slave robot and the master device .....	34
Figure 18. Kinematic representation of the reconstructed slave robot.....	35
Figure 19. Kinematic representation of the reconstructed master device.....	37
Figure 20. Comparison of the trajectories between master and slave about joint 2.....	42
Figure 21. Comparison of the trajectories between master and slave about joint 3.....	42
Figure 22. Comparison of the trajectories between master and slave about joint 4.....	43
Figure 23. Comparison of the trajectories between master and slave about joint 2 ( $\Theta_3 = 30^\circ$ ).....	43
Figure 24. Comparison of the trajectories between master and slave about joint 2 ( $\Theta_3 = 60^\circ$ ) .....	44
Figure 25. Simulation system for measuring trajectory of virtual master device and slave robot .....	45
Figure 26. Comparison of tragectories between virtual master and slave for four rotational joints.....	45

# I. INTRODUCTION

## 1.1 Introduction to Single Port Laparoscopic Surgery (SPLS)

The open surgery is the conventional method of an operation by generating a large operation wound in the abdominal area. Although the surgical difficulty of the open surgery for surgeons is low, this surgery impose a large burden on patient. Because of a large operation wound, it causes many amount of blood loss, large post-operative scar, a lot of complications and so on. In order to reduce this risk of the surgery, laparoscopic surgery which can decrease size of the operation wound by drilling three or four small holes has been conducted. The laparoscopic one offers for patients less bleeding amount, less post-operative scar, and shorter hospital stay compare with open surgery [1].

Moreover, thanks to ceaseless efforts to reduce the size and the number of the operation wound, single port laparoscopic surgery shortly SPLS had been developed as shown on figure 1. SPLS is an operation which leaves only one operation wound by inserting all surgical instruments through the navel inflated with CO<sub>2</sub>. Because of the one small operation wound, SPLS gives patients less post-operative scar, less risk of complications, and shorter hospital stay compare with open surgery and even multiport one [2]. One of the

greatest advantages of SPLS is that an operation wound is invisible because the surgery is conducted through the navel [3]. Furthermore, SPLS is able to cover wide range of operation such as partial nephrectomy [4], ureterolithotomy [5], single-port laparoscopic renal cryotherapy, radical nephrectomy, abdominal sacrocolpopexy, wedge kidney biopsy [6] and so on.

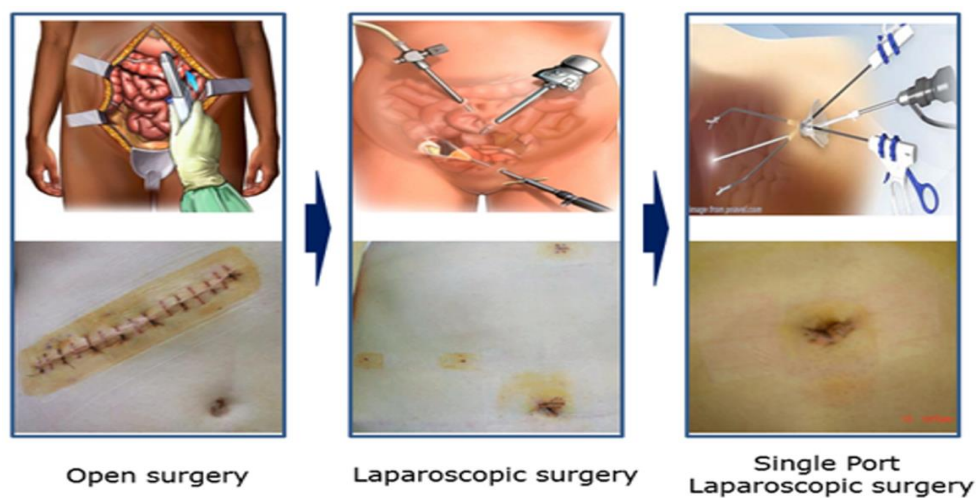


**Fig. 1** Development of surgical techniques and operation wounds

Although SPLS has many merits, the surgery require a lot of training and education time to surgeons [7]. Because long surgical instruments are intersected with a hole, it is difficult to manipulate the end of the instruments [2]. The instruments intersected like ‘X’ shape might lead counter-intuitive sense of direction for left and right hand. In addition, the surgery requires a high level concentration and long operation time for surgeon to avoid crashing instruments [8, 9, 10]. Owing to these technical challenges, surgeons are reluctant to conduct SPLS.

## 1.2 Previous researches of robotic SPLS

In order to address technical challenges of SPLS for surgeons, diverse master-slave systems have been developed. The master-slave system which consists of control and actuate part makes surgeons control the surgical robot by manipulating the master device at a comfortable place [11]. When surgeons manipulate the master device while watching the endoscopic image, the master device tracks the position and rotation of the surgeon's hands. After calculating the movement, the slave robot is operated. Figure 2 shows the master slave system for da Vinci system which is most commercialized in the world. The function of adjusting scale offered by the system prevents trembling the robot arm from hand tremor of the surgeon, and allows precise operation. For this advantage of the master-slave system, SPLS which requires long operation time and precise work in a confined abdominal space needs the system.

In case of the slave robot for SPLS, the types of the robots are mainly divided into X and Y type as shown on figure 3. The shape and intersected point of each character are the structure of the robot and an incision point such as the navel respectively. Although X-type robot provides the large workspace, it has a bulky structure. On the other hand, Y-type robot has a compact structure but the small workspace. X type robot is that two robot arms cross a hole like a 'X' shape. A typical example of the robot is da Vinci SI system

[12]. The robot of da Vinci SI system has two joint parts; one is responsible for translation on the outside of the body. The other is responsible for rotation in the body. As the robot originally designed for multi-port laparoscopic surgery, it has a bulky structure and lack of triangulation [13].

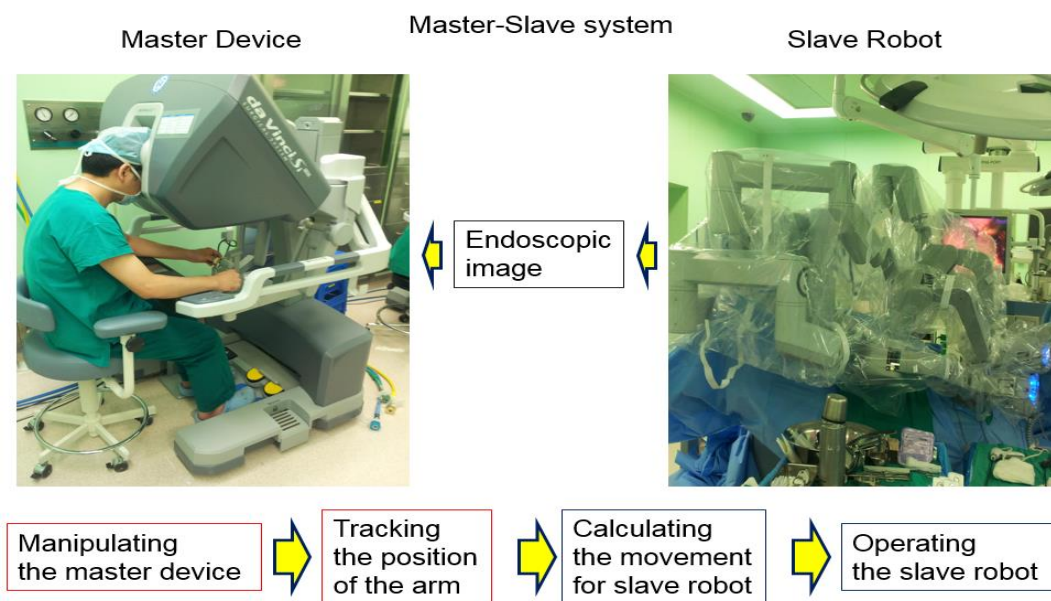


**Fig. 2** Master-Slave system for da Vinci SI

Owing to confined surgical environments, compact size of the robot is essential. Also triangulation of the robot should be secured to have various orientations of two forceps. In order to reduce the size of the robot and obtain the proper triangulation, ‘Y’ type robot has been developed. This robot has two phases in terms of its geometry which are ‘I’ and ‘Y’. The initial phase, ‘I’ is for insertion of the robot into one small incision. After insertion, two forceps are spread to form ‘Y’ shape. Unlike ‘X’ type robot equipped with motors at both ends, ‘Y’ type one has motors on the fixed one part as shown in figure 4. In case of ‘X’ type,

the motors have to be separated outside to get the triangulation. But, motors of the Y type robot does not have to be moved for triangulation, because 'Y' type robot has two joints for triangulation. Therefore 'Y' type one ensures proper triangulation with confined space. IREP [14], SPRINT [15], and PLAS [16] fall into 'Y' type robot. These robots have something in common that all joints inserted in the human body during the surgery.

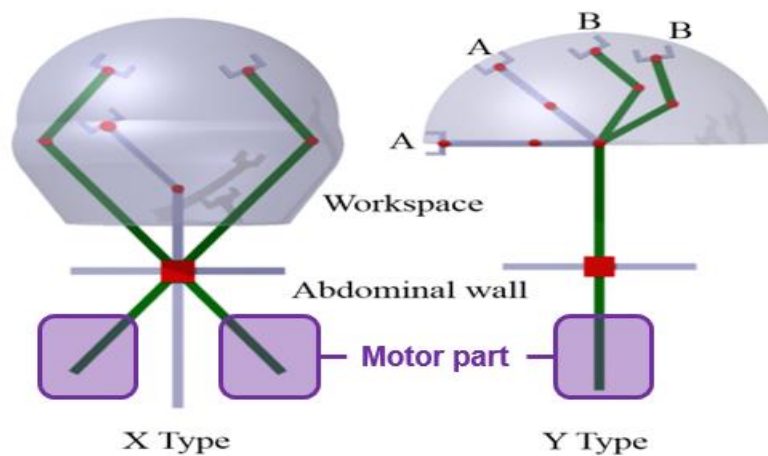
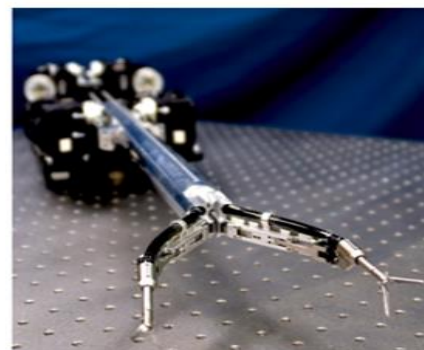


**Fig. 3** X-type and Y-type robot for SPLS



X-type slave robot



Y-type slave robot

**Fig. 4** X-type slave robot (da Vinci SI system) and Y-type slave robot (PLAS)

### 1.3 Previous researches of master device

In order to control the slave robot as surgeon's will, a master device is necessary. According to degree of freedom (DOF) and the aim of the slave robot, two types of the master device exist. The first type is to control the only tip of the robot by calculating the change of the rotations and translations such as the master device of da Vinci system [13]. PHANTOM OMNI [17] also falls into tip controlling master device. This type of master device allows operators to control slave robot intuitively since the tip of the slave robot follows the tip of the master device. The other type is to manipulate all joints of the robot separately by adopting joint to joint level control. The all joints controlling method is to control each joint contrast to the tip controlling method. An example of master used all joint controlling method is for exoskeleton [18]. In order to control the robot arm like a human arm, shoulder and elbow joint as well as wrist joint should be controlled. In the field of the surgical robot, all joints controlling method is applied to master device in Hyper Finger [19] and flexible endoscopic gastrointestinal robot manipulator [20]. Figure 5 shows tip controlling master device for da Vinci SI system [13] and all joints controlling master device for mutual telepresence [18].

For SPLS 'Y' type slave robot, all joints controlling master device is more suitable to control the

robot safely than tip controlling one. The reason is that all joints of the ‘Y’ type robot inserted in the human body during the surgery. Therefore, all joints as well as the tip of the robot should be manipulated to increase surgical safety. Otherwise, some joint operations will not be under control and may damage tissues. Also, we have to consider ergonomic design of master device. If we design master device with same structure of slave robot as a general method to control all joints, it might cause fatigue to the operators. Considering that SPLS requires high concentration and long operation time, ergonomic design should be adopted to reduce the fatigue of operators.

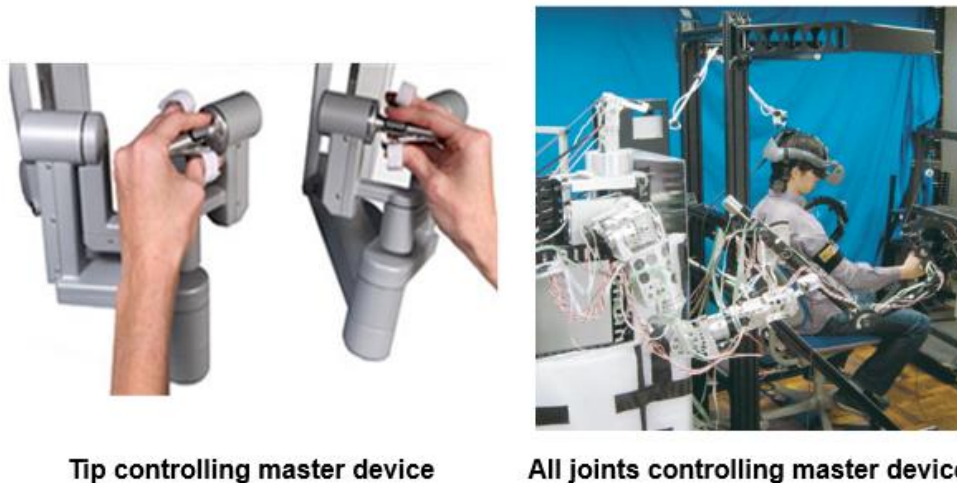


**Fig. 5** Tip controlling master device (da Vinci) and all joints controlling master device (TELESAR II)

## 1.4 Design factors of master device.

Before designing master device, several factors should be considered such as slave robot, ergonomics, sensors and material and so on. First, it is important for master design which slave robot will be manipulated. DOF of master device have to be greater than or equal to that of slave robot to use all joints of the robot. We also specified whether the slave robot requires tip controlling or all joints controlling method. If the motion at the end effector of slave robot is important, the master device should be designed to have dexterous workspace at the end effector of master device. If all joints of the robot should be manipulated separately, each joint of master device has to be corresponded to each joint of slave robot.

As a second factor, ergonomics should be considered for user convenience. Since SPLS requires long operation time and high concentration compare with other surgeries, we need the ergonomic master device to reduce the burden on the user. In case of all joint controlling master device, each joint of master device should be matched each joint of human arm. Especially, which joints of human arm will be chosen should be cautious. If three rotational joint will be placed at some joints of human arm, the wrist joint is best joints to spend the least amount of metabolism [21]. Furthermore, the angles of each joint have to be defined to manipulate the master device unconstrainedly. Also, in order to reduce the fatigue of the user as much as

possible, counterbalanced system is necessary. Using the system, we could not only maintain static balance but also minimize inertia of the master device. [22].

The third factor of the master design is sensors and material. Before deciding the sensors, we have to know which motion will be detected, how precise resolution will be required, and which size and weight is proper to the master device. Also, the master device should be made of the material which can withstand the force applied to the master device. Considering these design factors, we could make efficient and proper master device for the target robot.

## 1.5 Research contents and goals

In this study, the master device is designed for PLAS [16] which is one of the 'Y' type slave robot for SPLS. For the surgical safety, all joints controlling method is adopted to the master device because all joints of slave robot are inserted in the human body during the surgery. The sequence of design follows the design factors of master device as described above. Before designing master device, DOF and structure of slave robot must be analyzed. Then, according to ergonomics, joint matching among master, slave, and human arm, and link length should be determined. Also, motion range of the human arm have to be analyzed. This ergonomic design helps operators control the slave robot comfortably. In addition, counterbalanced system could minimize the fatigue of operators. Finally, sensors and material of master device will be specified to meet conditions.

After finishing the design, the method for all joints control should be considered. In order to have same velocities of the tips between master and slave by using simple 1:1 mapping factors, they should have same structure in the all joints control method. However, as the master device has different structure with slave robot for ergonomic design, we have to apply the special mapping factors to each joint. Therefore, we must find the mapping factors of all joints by using kinematics analysis. Then, we will confine whether the

velocity of the grip of the master device has similar that of slave robot by using MATLAB. Furthermore, we will verified they have similar trajectories at the same time by using simulation we designed.

The goal of this study lies in developing all joints controlling master device that can efficiently control the 'Y' type SPLS robot based on PLAS and ergonomics. Also, finding the mapping factors of all joints is the other aim to minimize trajectory error of tips between master and slave in the all joints controlling method.

## II. DESIGN CONSIDERATION OF MASTER DEVICE

### 2.1 Slave robot for Single Port Laparoscopic Surgery

To develop proper master device, analyzing a target slave robot is spade work. The target robot for SPLS is PLAS [16]. Conventional Y-type SPLS robots [14, 15] are not suitable to deal with relatively large organs such as intestine and liver, since the spreading point of two arms is fixed differ to manual SPLS and X-type SPLS robots as depicted on figure 6 [12]. In order to solve this problem, six degrees of freedom (DOFs) robot for each arm was developed, which consist of two prismatic joints at joint 1 and 5, and four rotational joints at joint 2, 3, 4, and 6, as shown on figure 7. The joint 1 provides a larger workspace by separating the starting division point of each arm. The joint 2 and 3 responsible for yaw joints are for making triangular position. The joint 4 and joint 6 correspond to pitch and roll joint respectively. The joint 5 is for forward and backward motion after determining orientation. Considering all the degrees of freedom of the individual arms, total 12 DOFs are realized in the design.

Kinematic representation of the left arm of the system is shown in figure 8, and its axes are labeled with respect to the distal Denavit - Hartenberg convention. The corresponding Denavit - Hartenberg parameters are also tabulated in Table 1.

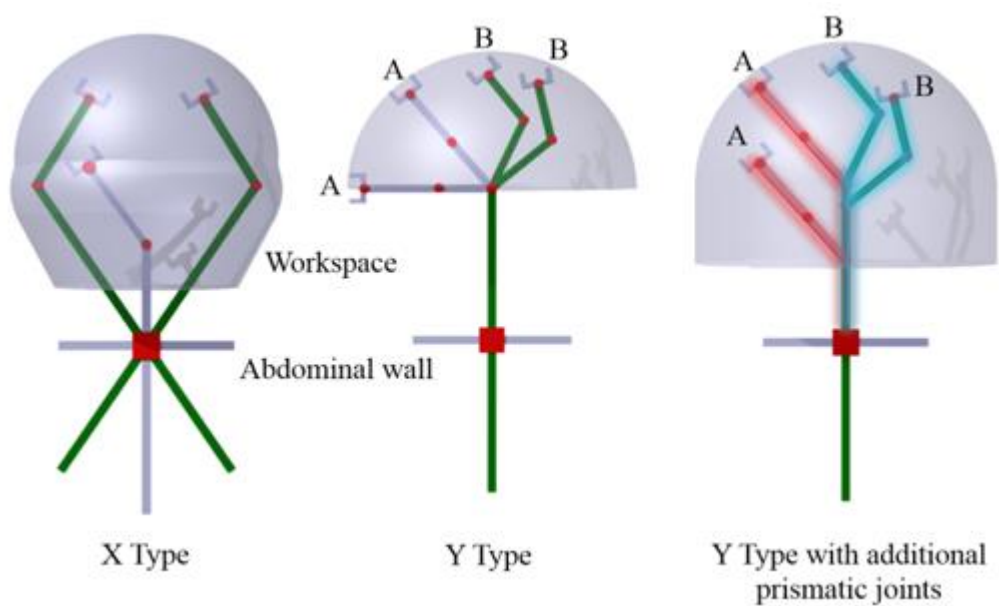


**Fig. 6** Type of robotic SPLS platform; X-type (left), Y-type (middle), PLAS (right)

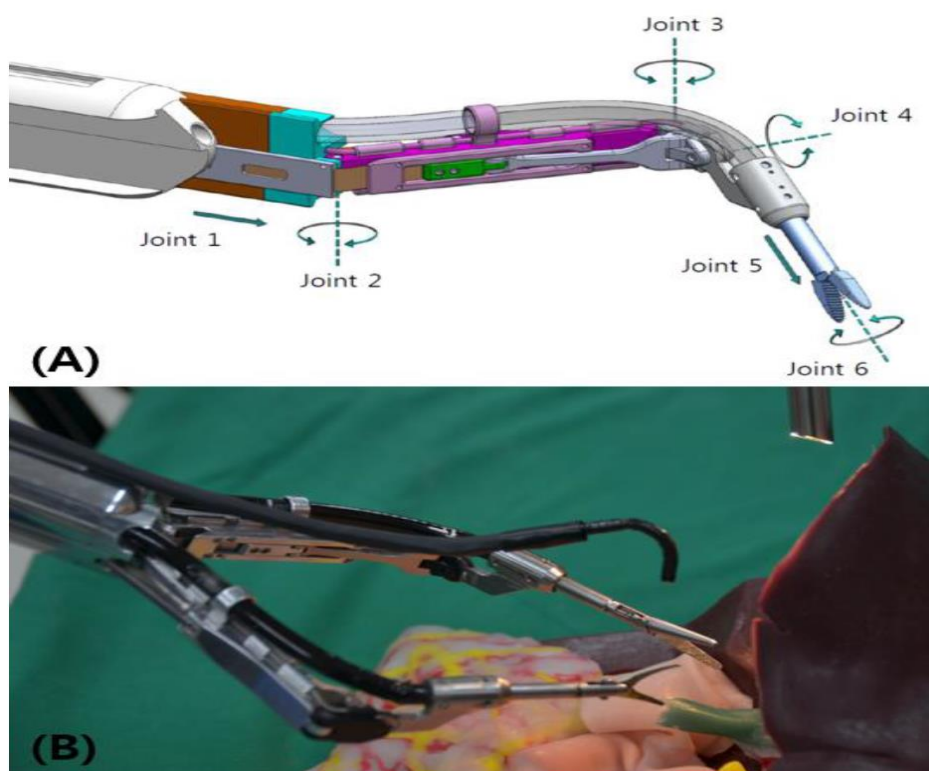


**Fig. 7** (A) CAD model and (B) prototype of PLAS

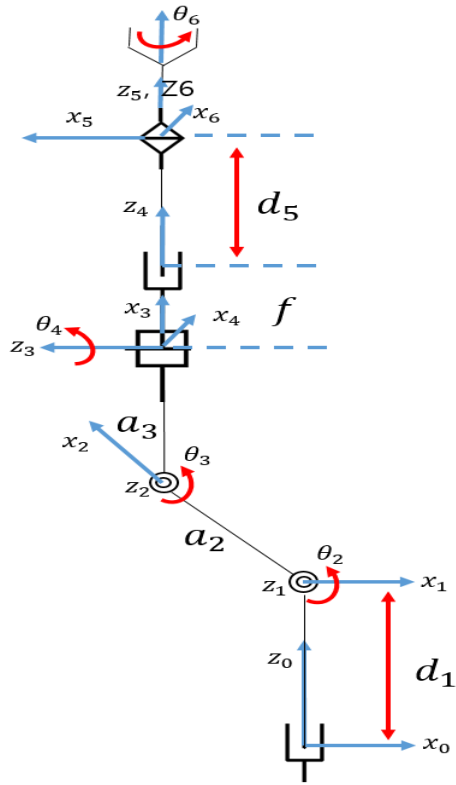


**Fig. 8** Kinematic representation of PLAS

**Table 1.** D-H parameters of PLAS

Joint i	$\alpha_i$	$a_i$	$d_i$	$\theta_i$
1	$\pi/2$	0	$d_1 = \text{variable}$	0
2	0	$a_2$	0	$\theta_2 = \text{variable}$
3	$3\pi/2$	$a_3$	0	$\theta_3 = \text{variable}$
4	$\pi/2$	0	0	$\theta_4 = \text{variable}$
5	0	0	$d_5 = \text{variable}$	0
6	0	0	$d_6$	$\theta_6 = \text{variable}$

## 2.2 Ergonomics

In order to manipulate the PLAS by using all joints controlling method, two yaw rotational joints, one pitch and roll rotational joint, and two prismatic joints are required in a master device. For controlling all joints separately, all joints of master device should correspond to each joint of human arm as well as that of slave robot. There are mainly two methods to match the joints between master device and human arm. First method is that two yaw joints correspond to the shoulder and elbow joint, and second method is that elbow and wrist joint are responsible for two yaw joints. In case of pitch and roll rotational joints, when they correspond to wrist joint, the fatigue of operators will be minimized [21]. The joint one is moved by forward and backward motion of shoulder, and joint five is manipulated by translation of the fingers.

Angles of each human joint should be analyzed to give operators comfort. If neutral angle of wrist is  $0^\circ$ , the wrist rotates from  $-70^\circ$  to  $60^\circ$  in flexion / extension and from  $-20^\circ$  to  $30^\circ$  in abduction/ adduction. In case of elbow joint, the angle of flexion is  $142^\circ$  and those of supination / pronation are  $90^\circ$  and  $80^\circ$  as a maximal value [23]. When the master device is designed, this ergonomic factors should be considered.

### 2.1.1 Joint arrangement

The first design of master device was considered that slave robot has offset length between yaw and pitch rotational joint [24]. The designed master device provides six DOFs of movement to manipulate the six DOFs of the slave robot. The CAD and kinematic model of the proposed master device are depicted on Fig 9 and the Denavit–Hartenberg parameters are given as shown on Table 2. The overall size of each master device is approximately 15 cm by 14 cm by 24 cm. Each joint of the master device corresponds to each joint of human arm, enabling separate control of each joint. First, the joint 1 takes charge of the forward and backward motion of the shoulder. Second, the joint 2 and 3 are in charge of the rotational motions of the shoulder and the elbow respectively. These two joints allow the slave robot to have triangulation. Third, joint 4 takes charge of the forward and backward motion of fingers. Last, joint 5 and 6 are used for flexion / extension and rotation of the wrist. This joint to joint correspondence enables the whole part of slave robot to move as desired.

**Table 2.** D-H parameters of the first master device

i	$\alpha_i$ (degrees)	$a_i$ (mm)	$d_i$ (mm)	$\Theta_i$ (degrees)
1	$\pi/2$	20	$d_1$	0
2	$\pi/2$	0	$d_2$	90
3	$\pi/2$	0	80	$\Theta_2+90$
4	$-\pi/2$	0	$d_4+35$	90
5	$\pi/2$	0	0	$\Theta_5$
6	0	0	80	$\Theta_6$

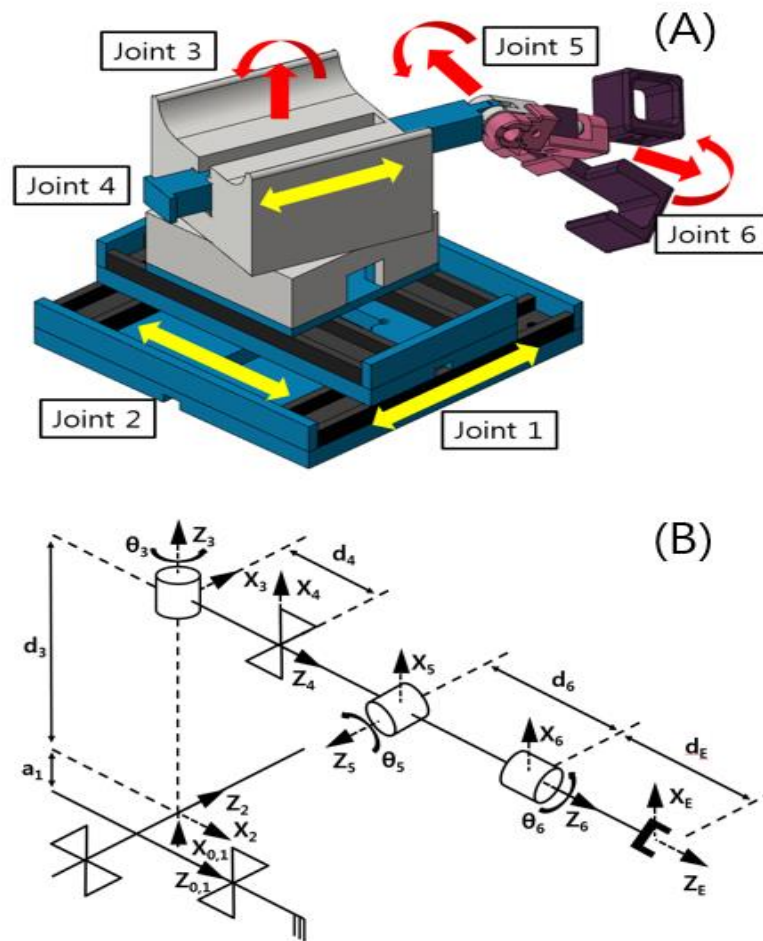


**Fig. 9** (A) CAD and (B) kinematic model of the first master device for Y-type SPLS robot

Although all joints can be controlled separately through the first version of master device, user easily get a fatigue because of different joint structure between master device and human arm and using whole arm from shoulder to wrist. In order to reduce the fatigue of operators, the second version of master device has been developed more ergonomically. The joint 1 takes charge of the forward and backward motion of the shoulder similar to first version. But it is changed from position control method to switch

method. The reason is that position control by using 1 by 1 matching might give operators the burden because the range of joint 1 is too wide from 0 to 215 mm. The joint 2 and 3 which are in charge of rotational motion of the elbow and the wrist joint differ to the first version manipulated by the shoulder and the elbow joint. Because of no length offset between joint 3 and 4, three rotational joint which are joint 3, 4, and 6 are placed at one point wrist joint. It makes motion of operators be dexterous without restriction. The joint 5 is manipulated by translation of fingers. Also, joint 2 is the role of armrest to support the weight of the arm. The CAD model of the proposed master device are depicted on Fig 10.

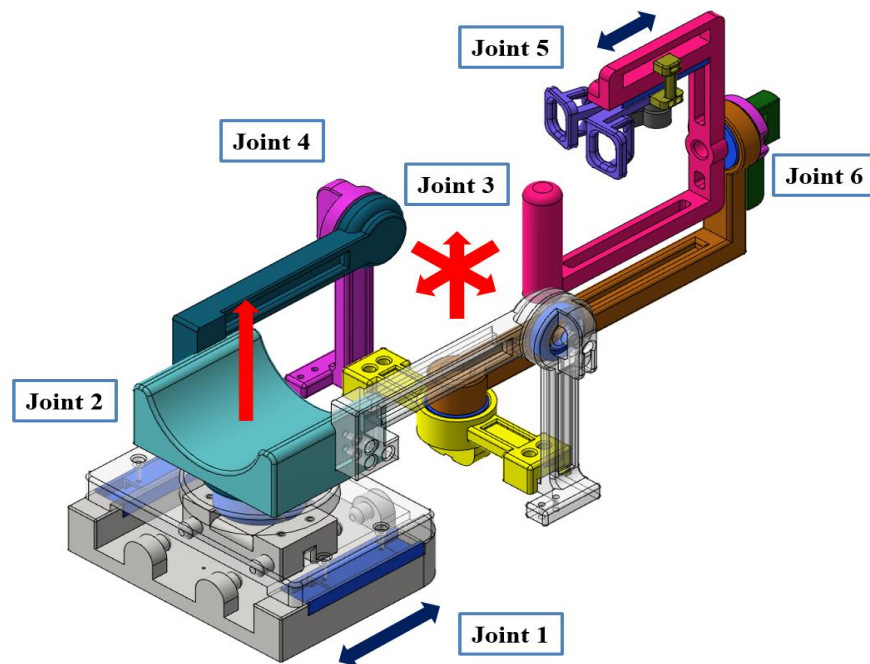


**Fig. 10** CAD model of the second master device for Y-type SPLS robot

### 2.1.2 Balance of the positioning stage

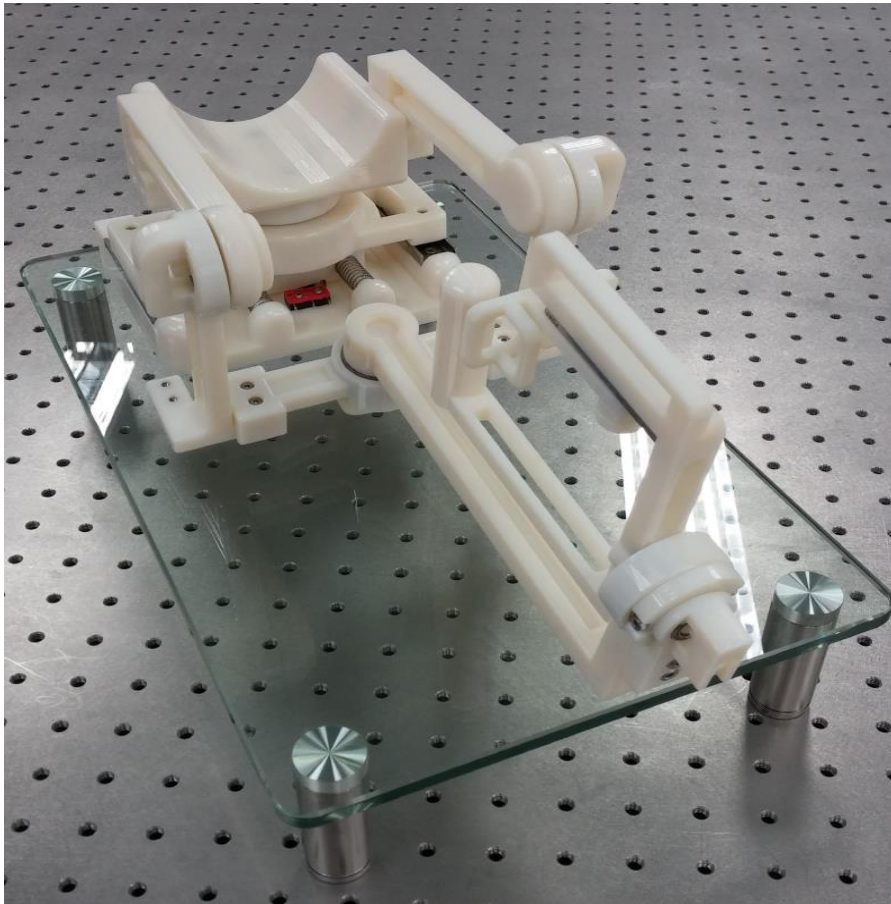


**Fig. 11** Prototype of the second master device for Y-type SPLS robot

The second version of master device has been developed considering ergonomics as shown on figure 11. Because three rotational joints are placed at wrist joint, the master device could be manipulated without restriction. However, due to the weight of the links after joint 4, it is hard to rotate the joint 4 as a pitch rotation of wrist. As the weight of links after joint 4 is about 240g, the joint is tilted approximately 60 degrees as shown in Figure 12. Given that the wrist is rotated on average from 0 to 50 in abduction / adduction, users always withstand the weight. Therefore, it might give the burden to users for a long time. In order to

reduce this burden, joint 4 should be tilted about 25 degrees in steady state.

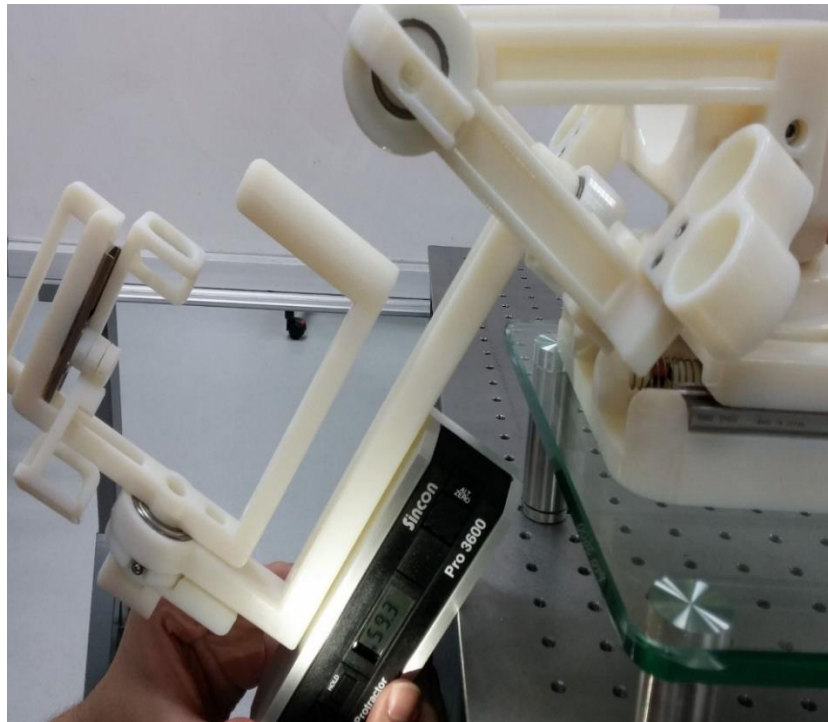


**Fig. 12** Angle of joint 4 without counterbalancing



**Fig. 13** A simple schematic drawing of the positioning stage

In order to keep a balance at a joint, positioning stage which is counterbalancing is required. A simple schematic drawing about staging position is depicted on Fig 13. After obtaining parameters  $M$  and  $L$  from weight and link length of master device,  $m$  and  $l$  are set based on the pivot point for gravity compensation. For the positioning stage, the equation of  $ML = ml$  should be satisfied. In addition, when  $m$  has

maximum weight, the master device will have lowest inertia according to the equation of  $I = ML^2 + ml^2$

$= ML^2 \left( \frac{M}{m} + 1 \right)$  [22]. To obtain 25 degrees at joint 4 in steady state, a schematic drawing is depicted on Fig

14.

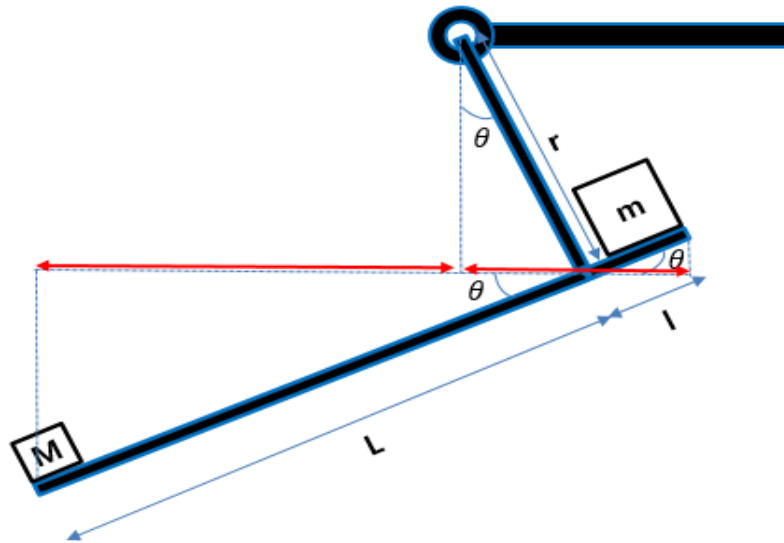


**Fig. 14** A simple schematic drawing of the positioning stage about joint 4

Based on joint 4 as a pivot joint,  $M$  and  $L$  are weight and link length of master device, and  $m$  and  $l$  are those of counterbalancing part. Considering that the maximum weight of  $m$  yields the lowest inertia, the master device has two counterbalancing part. The values of parameters are as follows:  $r = 9$  cm,  $M = 240.5$  g,  $L = 18.8$  cm,  $l = 3.4$  cm.

$$m(r\sin\theta + l\cos\theta) = M(L\cos\theta - r\sin\theta) \tag{1}$$

$$m = \frac{M(L\cos\theta - r\sin\theta)}{(r\sin\theta + l\cos\theta)}$$

From (1),  $2m$  is about 460g. By setting two counterbalancing parts 260g on either side of the joint

4, it was confirmed that joint 4 is tilted about 25 degrees in steady state as shown in Fig 15.

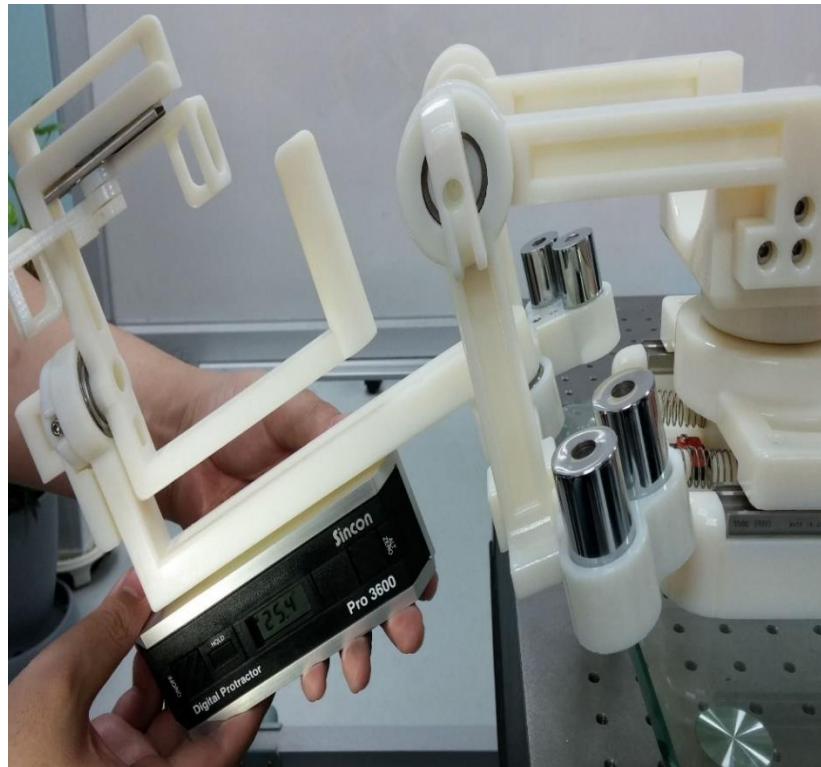


**Fig. 15** Angle of joint 4 with conterbalancing

## 2.3 Sensors and material

In order to detect the motion of operator's arm from the master device, sensors are required as many as the number of joints of the master device. The master device consists of two prismatic and four rotational joints. As shown in figure 10, the joint 1 is detected by on/off switch because the range of joint 1 is too wide to control by using 1 by 1 matching. As sensors of the rotational joints from joint 2 to joint 5, Ultra Miniature size Encoder 7S series from Nemicon is selected. The encoder has high resolution up to 400 and small size that the diameter of the encoder is 7.2 pie and the height is 13.5 mm. The weight of the sensor is light enough to manipulate the master device without significant impact. In case of joint 6 as a prismatic joint, a linear potentiometer is used.

All parts of the master device are made by using 3D printing system from Eden 250<sup>TM</sup>. It has 16 micron high resolution. As a material, we used FullCure 835 from Objet which has 57 MPa of tensile strength and 2,220 MPa of modulus of elasticity as the minimum value. The material has sufficient strength to manipulate the master device by the human arm.

### III. KINEMATICS ANALYSIS AND MAPPING FACTORS

In case of the tip control master device, it makes the tip of the slave robot move along the tip of the master device by using kinematics. After calculating change of rotations and translations from forward kinematics of master device, through the inverse kinematics of slave robot the tip of the robot is controlled.

In case of the general all joints controlling master device, it makes each joint of the slave robot follow each joint of the master device. However, if the structure between the slave robot and the master device is different, the joint control method only 1 by 1 matching might have different trajectory between them. In order to minimize the trajectory error, the proper mapping factors must be found. Through the Jacobians of the master device and slave robot, the mapping factors could be calculated to have similar velocity of the tip between the master and slave as much as possible.

Throughout this section, forward kinematics, inverse kinematics, and Jacobian of the left master device will be analyzed. Kinematic representation of the left master device is shown in figure 16, and its axes are labeled with respect to the distal Denavit - Hartenberg convention. The corresponding Denavit - Hartenberg parameters are also tabulated in Table 3.

The transformation matrix between the  $i_{th}$  and the  $(i-1)_{th}$  coordinate system can be obtained by translating

$(i-1)$ th coordinate system along the  $z_{i-1}$  axis by  $d_i$ , rotating the resulting system around  $z_{i-1}$  axis by  $\theta_i$ , translating resulting system along the  $x_i$  axis by  $a_i$ , and finally rotating the resulting system around  $x_i$  axis by  $\alpha_i$ , (1).

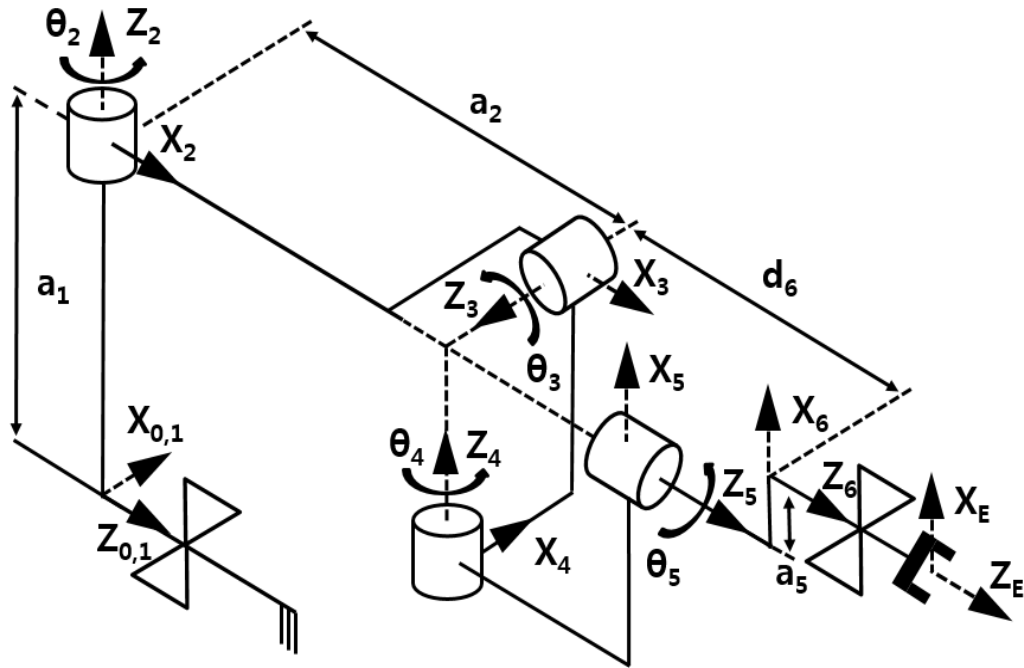


**Fig. 16** Kinematic representation of the designed master device

**Table 3.** D-H parameters of the designed master device

Joint i	$\alpha_i$	$a_i$	$d_i$	$\theta_i$
1	0	0	$d'_1 = \text{variable}$	0
2	$-\pi/2$	$a_1$	0	$-90 + \theta_2 = \text{variable}$
3	$\pi/2$	$a_2$	0	$\theta_3 = \text{variable}$
4	$-\pi/2$	0	0	$90 + \theta_4 = \text{variable}$
5	$\pi/2$	0	0	$90 + \theta_5 = \text{variable}$
6	0	$a_5$	$d_6 + d'_6 = \text{variable}$	0

$${}^{i-1}T_i = T(z_{i-1}, d_i)T(z_{i-1}, \theta_i)T(x_i, a_i)T(x_i, \alpha_i) \quad (2)$$

where,

$$T(z_{i-1}, d_i) = \begin{bmatrix} 1 & 0 & 0 & 0 \\ 0 & 1 & 0 & 0 \\ 0 & 0 & 1 & d_i \\ 0 & 0 & 0 & 1 \end{bmatrix}, \quad T(z_{i-1}, \theta_i) = \begin{bmatrix} C_i & -S_i & 0 & 0 \\ S_i & C_i & 0 & 0 \\ 0 & 0 & 1 & 0 \\ 0 & 0 & 0 & 1 \end{bmatrix},$$

$$T(x_i, a_i) = \begin{bmatrix} 1 & 0 & 0 & a_i \\ 0 & 1 & 0 & 0 \\ 0 & 0 & 1 & 0 \\ 0 & 0 & 0 & 1 \end{bmatrix}, \quad T(x_i, \alpha_i) = \begin{bmatrix} 1 & 0 & 0 & 0 \\ 0 & C\alpha_i & -S\alpha_i & 0 \\ 0 & S\alpha_i & C\alpha_i & 0 \\ 0 & 0 & 0 & 1 \end{bmatrix}$$

And  $C_i = \cos \theta_i$ ,  $S_i = \sin \theta_i$ ,  $C\alpha_i = \cos \alpha_i$ , and  $S\alpha_i = \sin \alpha_i$ . Multiplying the matrices in order with re-

spect to the (1)  ${}^{i-1}T_i$  can be expanded as,

$${}^{i-1}T_i = \begin{bmatrix} C_i & -C\alpha_i S_i & S\alpha_i S_i & a_i C_i \\ S_i & C\alpha_i C_i & -S\alpha_i C_i & a_i S_i \\ 0 & S\alpha_i & C\alpha_i & d_i \\ 0 & 0 & 0 & 1 \end{bmatrix} \quad (3)$$

In order to calculate the final transformation matrix  ${}^0T_6$  between the floating coordinate system of the end effector and the fixed ground global coordinate system of the manipulator, series of matrix multiplications should be carried out.

$${}^0T_6 = {}^0T_1 {}^1T_2 {}^2T_3 {}^3T_4 {}^4T_5 {}^5T_6 \quad (4)$$

Substituting the D-H parameters in Table 1 to (3) and using (4)  ${}^0T_6$  will be calculated as,

$${}^0T_6 = \begin{bmatrix} u_x & v_x & w_x & p_x \\ u_y & v_y & w_y & p_y \\ u_z & v_z & w_z & p_z \\ 0 & 0 & 0 & 1 \end{bmatrix} \quad (5)$$

where,

$$u_x = (S_2C_4 + C_2C_3S_4)S_5 - C_2S_3C_5, \quad u_y = -(C_2C_4 + S_2C_3S_4)S_5 - S_2S_3C_5, \quad u_z = S_3S_4S_5 + C_3C_5,$$

$$v_x = (S_2C_4 + C_2C_3S_4)C_5 + C_2S_3S_5, \quad v_y = -(C_2C_4 + S_2C_3S_4)C_5 + S_2S_3S_5, \quad v_z = S_3S_4C_5 - C_3S_5,$$

$$w_x = C_2C_3C_4 - S_2S_4, \quad w_y = S_2C_3C_4 + C_2S_4, \quad w_z = S_3C_4,$$

$$p_x = a_2C_2 - d_6(S_2S_4 - C_2C_3C_4), \quad p_y = a_2S_2 + d_6(C_2S_4 - S_2C_3C_4), \quad p_z = d_6S_3C_4$$

### 3.1 Forward kinematics

The objective of the direct kinematics is to find the manipulator end effector location that includes both position and orientation by giving the values of the joint angles for revolute pairs and the joint translation amounts for prismatic pairs. Any position vector represented in end effector coordinate system

${}^6q = [{}^6q_x, {}^6q_y, {}^6q_z, 1]^T$  can be expressed in the fixed ground global coordinate system

${}^0q = [{}^0q_x, {}^0q_y, {}^0q_z, 1]^T$  by using the transformation matrix  ${}^0T_6$  in the formulation,

$${}^0q = {}^0T_6 {}^6q \quad (6)$$

As the point p is the origin of the end effector coordinate system  ${}^6p = [0, 0, 0, 1]^T$ , the end effector position expressed in the fixed ground global coordinate system will be the last column of the transformation

matrix  ${}^0T_6$ ,  ${}^0p = [p_x, p_y, p_z, 1]^T$ . Also the orientation of the end effector can be represented by the three

unit vectors  $(u_x, u_y, u_z)$ ,  $(v_x, v_y, v_z)$ , and  $(w_x, w_y, w_z)$  as they form the rotation matrix inside the trans-

formation matrix,

$${}^0T_6 = \begin{bmatrix} [{}^0R_6]_{3 \times 3} & [{}^0p]_{3 \times 1} \\ [0]_{1 \times 3} & 1 \end{bmatrix} \quad (7)$$

## 3.2 Inverse kinematics

The objective of the inverse kinematics is to find the joint angles for revolute pairs and the joint translation amounts for prismatic pairs by giving the location of the end effector. As the values of the trans-

formation matrix  ${}^0T_6$  components are given, variable joint parameters  $\theta_2, \theta_3, \theta_4$ , and  $\theta_5$  can be calculated by

modifying (4) as follows,

$${}^0T^{-1}{}^0E = {}^2T^3{}^4T^5T^E \quad (8)$$

here,

$${}^0T^{-1}{}^0E = \begin{bmatrix} r_{11}C_2 + r_{21}S_2 & r_{12}C_2 + r_{22}S_2 & r_{13}C_2 + r_{23}S_2 & p_xC_2 + p_yS_2 \\ r_{21}C_2 - r_{11}S_2 & r_{22}C_2 - r_{12}S_2 & r_{23}C_2 - r_{13}S_2 & p_yC_2 - p_xS_2 \\ r_{31} & r_{32} & r_{33} & p_z \\ 0 & 0 & 0 & 1 \end{bmatrix} \quad (9)$$

$${}^2T^3{}^4T^5T^E = \begin{bmatrix} C_3S_4S_5 - S_3C_5 & S_3S_5 - C_3S_4C_5 & C_3C_4 & a_2 + d_6C_3C_4 \\ -C_4S_5 & -C_4C_5 & S_4 & d_6S_4 \\ C_3C_5 + S_3S_4S_5 & S_3S_4C_5 - C_3S_5 & S_3C_4 & d_6S_3C_4 \\ 0 & 0 & 0 & 1 \end{bmatrix}$$

As  $\theta_2$  is known from (8) and (9),

$$-p_x \sin(\theta_2) + p_y \cos(\theta_2) = d_6 \sin(\theta_4) \quad (10)$$

$$-r_{13} \sin(\theta_2) + r_{23} \cos(\theta_2) = \sin(\theta_4)$$

and,

$$\tan(\theta_2) = \frac{p_y - d_6 r_{23}}{p_x - d_6 r_{13}} = k \quad (11)$$

$$\theta_2 = \arctan2(k, \pm \sqrt{1 - k^2})$$

In order to proceed further in the calculation of remaining variable parameters,  $\theta_3$  and  $\theta_5$  can be solved by

using (11) as below,

$$\tan(\theta_3) = \frac{r_{33}}{r_{13} \cos(\theta_2) + r_{23} \sin(\theta_2)} = k_3 \quad (12)$$

$$\theta_3 = \arctan2(k_3, \sqrt{1 - k_3^2})$$

and,

$$\tan(\theta_5) = \frac{r_{21}\cos(\theta_2) - r_{11}\sin(\theta_2)}{r_{22}\cos(\theta_2) - r_{12}\sin(\theta_2)} = k_1 \quad (13)$$

$$\theta_5 = \arctan2(k_1, \sqrt{1 - k_1^2})$$

After the calculation of  $\theta_2$  and  $\theta_5$ ,  $\theta_4$  be found by using (8),

$$\sin(\theta_4) = r_{23}\cos(\theta_2) - r_{13}\sin(\theta_2),$$

$$\cos(\theta_4) = \frac{-r_{21}\cos(\theta_2) + r_{11}\sin(\theta_2)}{\sin(\theta_5)} \quad (14)$$

$$\tan(\theta_4) = k_2$$

$$\theta_4 = \arctan2(k_2, \sqrt{1 - k_2^2})$$

It should be noted that there exist multiple solutions for the inverse kinematics problem. In order to reduce the number of solutions, atan2 function can also be used where possible.

### 3.3 Jacobian

The objective of the direct kinematics is to find the manipulator end effector location that includes both position and orientation by giving the values of the joint angles for revolute pairs and the joint translation amounts for prismatic pairs. Any position vector represented in end effector coordinate

Velocity components of the end effector in the designed master device can be carried out by using

the joint rates,

$$\begin{bmatrix} v_6 \\ w_6 \end{bmatrix} = J \begin{bmatrix} d'_1 \\ \theta'_2 \\ \theta'_3 \\ \theta'_4 \\ \theta'_5 \\ d'_6 \end{bmatrix} \quad (15)$$

where,  $v_6$  is the linear velocity of the origin of the end effector coordinate system,  $v_6 = [v_{6x} \ v_{6y} \ v_{6z}]^T$ ,

$w_6$  is the angular velocity of the end effector,  $w_6 = [w_{6x} \ w_{6y} \ w_{6z}]^T$ , and  $J_{6 \times 6}$  is a Jacobian matrix

that transforms the actuated joint rates in the actuator space to the velocity state in the end effector space.

The Jacobian matrix  $J$  can be subdivided into  $J_1$  and  $J_2$ , and (19) can be modified as,

$$\begin{bmatrix} v_6 \\ w_6 \end{bmatrix} = \begin{bmatrix} J_1 \\ J_2 \end{bmatrix} \begin{bmatrix} d'_1 \\ \theta'_2 \\ \theta'_3 \\ \theta'_4 \\ \theta'_5 \\ d'_6 \end{bmatrix} \quad (16)$$

where,

$$J_1 = \begin{bmatrix} \frac{\partial p_x}{\partial d_1} & \frac{\partial p_x}{\partial \theta_2} & \frac{\partial p_x}{\partial \theta_3} & \frac{\partial p_x}{\partial \theta_4} & \frac{\partial p_x}{\partial \theta_5} & \frac{\partial p_x}{\partial d_6} \\ \frac{\partial p_y}{\partial d_1} & \frac{\partial p_y}{\partial \theta_2} & \frac{\partial p_y}{\partial \theta_3} & \frac{\partial p_y}{\partial \theta_4} & \frac{\partial p_y}{\partial \theta_5} & \frac{\partial p_y}{\partial d_6} \\ \frac{\partial p_z}{\partial d_1} & \frac{\partial p_z}{\partial \theta_2} & \frac{\partial p_z}{\partial \theta_3} & \frac{\partial p_z}{\partial \theta_4} & \frac{\partial p_z}{\partial \theta_5} & \frac{\partial p_z}{\partial d_6} \end{bmatrix} \quad (17)$$

Using (5) and (17),

$$J_1 = \begin{bmatrix} 0 & -a_2 S_2 - d_6 (C_2 S_4 + S_2 C_3 C_4) & -d_6 C_2 S_3 C_4 & -d_6 (S_2 C_4 + C_2 C_3 S_4) & 0 & 0 \\ 0 & a_2 C_2 + d_6 (-S_2 S_4 - C_2 C_3 C_4) & d_6 S_2 S_3 C_4 & d_6 (C_2 C_4 + S_2 C_3 S_4) & 0 & 0 \\ 1 & 0 & d_6 C_3 C_4 & -d_6 S_3 S_4 & 0 & 1 \end{bmatrix} \quad (18)$$

$\mathbf{J}_2$  can be computed by using the rotation matrix  ${}^0R_6$  and calculating  $w_6 = [w_{6x} \ w_{6y} \ w_{6z}]^T$ .

Taking the time derivative of  ${}^0R_6$  and multiplying the result with  ${}^0R_6^{-1}$  will result in a skew matrix.

$$\frac{\partial {}^0R_6}{\partial t} ({}^0R_6)^{-1} = \Omega \quad (19)$$

where,

$$\Omega = \begin{bmatrix} 0 & -w_{6z} & w_{6y} \\ w_{6z} & 0 & -w_{6x} \\ -w_{6y} & w_{6x} & 0 \end{bmatrix} \quad (20)$$

Using (5), (7), (19) and (20), angular velocity components of the end effector can be calculated and the

second portion of the Jacobian matrix  $\mathbf{J}_2$  will be,

$$J_2 = \begin{bmatrix} 0 & 0 & S_2 & -C_2S_3 & C_2C_3C_4 - S_2S_4 & 0 \\ 0 & 0 & -C_2 & -S_2S_3 & S_2C_3C_4 + C_2S_4 & 0 \\ 0 & 1 & 0 & C_3 & S_3C_4 & 0 \end{bmatrix} \quad (21)$$

As the Jacobian matrix of the master device is known, from this point velocity analysis can easily be car-

ried out. Also by analyzing the Jacobian matrix, singular configurations of the manipulator can also be

computed.

### 3.4 Mapping factors

In case of Y-type robotic SPLS, since all joints of robot are inserted in the human body during surgery, a master device is necessary to control all joints of the slave robot separately. When we design all joints controlling master device, the joints of slave robot and that of human arm should be considered to match with the joints of master device. If a master device is designed to be same structure of slave robot, the tip of the slave robot can be controlled by manipulating each joints. But, because of different structure between master device and human arm, manipulating the master device might lead to fatigue. Considering that SPLS requires high concentration and long operation time, ergonomic design of master device which is correspond to structure of the human arm as well as that of the slave robot. When the master device is designed by considering the structure of human arm unlike slave robot, generally the method of inverse Jacobian  $\Theta'_S = J_S^{-1}v_M$  is used to get the same velocities between tips of master device and slave robot. Although they could have the same velocities by using inverse Jacobian, the method might not apply to the all joints controlling master device. The reason is that if we use the inverse Jacobian, some joints of slave robot could be coupled and we can not control each joint separately. Therefore, in order to have similar velocities of tips between master and slave as much as possible in the all joints controlling method, the mapping factors of each joints will be found in this section. In summary, the aim is to not only design all

joints controlling master device ergonomically, but also control tip velocity of the slave robot as can as similar to that of master device.

Mapping factors for four revolute joints are found except prismatic joints joint 1 and 5. In case of prismatic joints, mapping factors of them are easily found such as on / off switching and simple 1:1 mapping. In contrast, mapping factors for rotational joints joint 2, 3, 4, and 6 should be calculated because of different structure between master and slave. In order to find these mapping factors, each Jacobian of them is found from joint 2 as a start joint to pillar part as end effector as shown on figure 17.

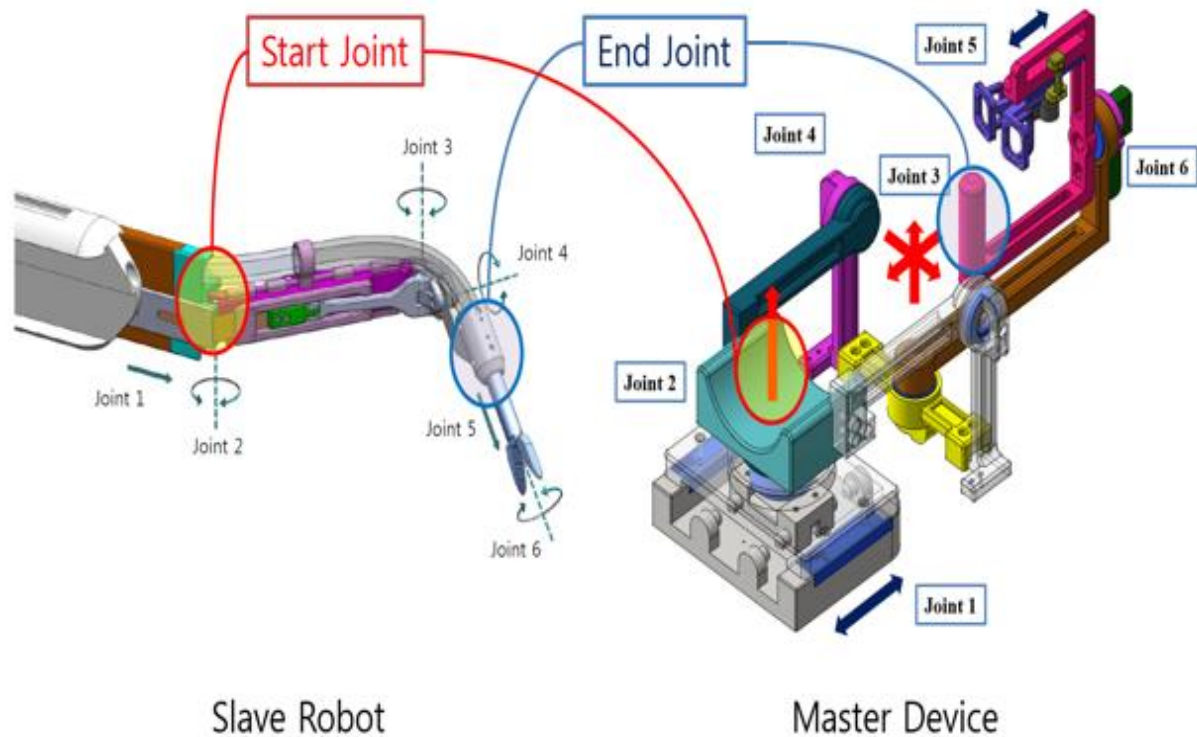


**Fig. 17** Start and end joint of the slave robot and the master device

The kinematics model and D-H parameters of slave robot are reconstructed as shown in figure 18

and on table4. In order to get the velocity of the end effector in figure 18, Jacobian is found as follows,

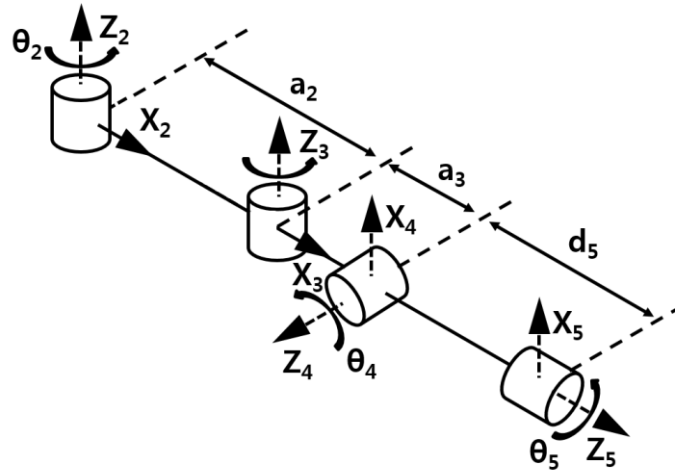


**Fig. 18** Kinematic representation of the reconstructed slave robot

**Table 4.** D-H parameters of the reconstructed slave robot

Joint i	$\alpha_{i-1}$	$a_{i-1}$	$d_i$	$\theta_i$
2	0	0	0	$\theta_2$
3	0	$a_2$	0	$\theta_3$
4	$\pi/2$	$a_3$	0	$\theta_4+90$
5	$\pi/2$	0	$d_5$	$\theta_5$

${}^0T_E$  is calculated as,

$${}^0T_E = \begin{bmatrix} r_{11} & r_{12} & r_{13} & p_x \\ r_{21} & r_{22} & r_{23} & p_y \\ r_{31} & r_{32} & r_{33} & p_z \\ 0 & 0 & 0 & 1 \end{bmatrix} \quad (22)$$

where,

$$p_x = a_3(C_2C_3 - S_2S_3) + a_2C_2 + d_5C_4(C_2C_3 - S_2S_3)$$

$$p_y = a_3(C_2S_3 + S_2C_3) + a_2S_2 + d_5C_4(C_2S_3 + S_2C_3)$$

$$p_z = d_5S_4$$

The Jacobian matrix is found as,

$${}^0J_E = \begin{bmatrix} {}^0v_E \\ {}^0w_E \end{bmatrix} = \begin{bmatrix} \frac{\partial {}^0P_{Eorg}}{\partial \theta_2} & \frac{\partial {}^0P_{Eorg}}{\partial \theta_3} & \frac{\partial {}^0P_{Eorg}}{\partial \theta_4} & \frac{\partial {}^0P_{Eorg}}{\partial \theta_5} \\ {}^0Z_2 & {}^0Z_3 & {}^0Z_4 & {}^0Z_5 \end{bmatrix} \quad (23)$$

Velocity components of the end effector can be carried out in joint rates,

$$\begin{bmatrix} v_6 \\ w_6 \end{bmatrix} = J \begin{bmatrix} \theta'_2 \\ \theta'_3 \\ \theta'_4 \\ \theta'_5 \end{bmatrix} \quad (24)$$

Using (22), (23), and (24), velocity components of the end effector can be calculated in the reconstructed slave

robot.

$$v_x = (-S_{23}(a_3 + d_5C_4) - a_2S_2)\Theta'_2 + (-S_{23}(a_3 + d_5C_4))\Theta'_3 + (-d_5S_4C_{23})\Theta'_4$$

$$v_y = (C_{23}(a_3 + d_5C_4) + a_2C_2)\Theta'_2 + (C_{23}(a_3 + d_5C_4))\Theta'_3 + (-d_5S_4S_{23})\Theta'_4 \quad (25)$$

$$v_z = (d_5C_4)\Theta'_4$$

The kinematics model and D-H parameters of master device also are reconstructed as shown in

figure 19 and on table5. In figure 15, joint 6 means handle part as end effector. In order to get the velocity

of the end effector, Jacobian is found as follows,

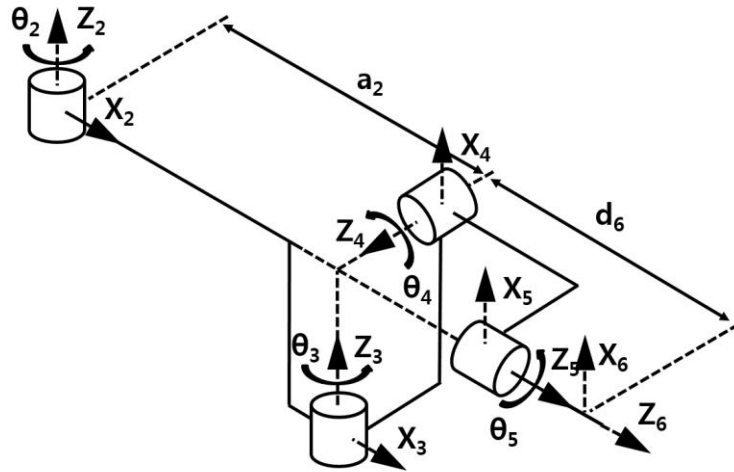


**Fig. 19** Kinematic representation of the reconstructed master device

**Table 5.** D-H parameters of the reconstructed master device

Joint i	$\alpha_{i-1}$	$a_{i-1}$	$d_i$	$\theta_i$
2	0	0	0	$\theta_2$
3	0	$a'_2$	0	$\theta_3$
4	$\pi/2$	0	0	$\theta_4+90$
5	$\pi/2$	0	0	$\theta_5$
6	0	0	$d_6$	0

${}^0T_E$  is calculated using (22),

$$p_x = a_2 C_2 + d_6 C_4 (C_2 C_3 - S_2 S_3)$$

$$p_y = a_2 S_2 + d_6 C_4 (C_2 S_3 + S_2 C_3)$$

$$p_z = d_6 S_4$$

Using (22), (23), and (24), velocity components of the end effector can be calculated in the reconstructed master device.

$$\begin{aligned} v_x &= (-S_{23}(d_6 C_4) - a'_2 S_2) \Theta'_2 + (-S_{23}(d_6 C_4)) \Theta'_3 + (-d_6 S_4 C_{23}) \Theta'_4 \\ v_y &= (C_{23}(d_6 C_4) + a'_2 C_2) \Theta'_2 + (C_{23}(d_6 C_4)) \Theta'_3 + (-d_6 S_4 S_{23}) \Theta'_4 \\ v_z &= (d_6 C_4) \Theta'_4 \end{aligned} \quad (26)$$

In order to have similar velocities of end effectors between master device and slave robot, (25) and (26) should be same as much as possible. From this equation we can get relationships of each joint velocity between master device and slave robot as follow,

$$\begin{aligned} (d_5) \Theta'_{4(\text{slave})} &= (d_6) \Theta'_{4(\text{master})} \\ (a_3 + d_5 C_4) \Theta'_{3(\text{slave})} &= (d_6 C_4) \Theta'_{3(\text{master})} \\ (C_{23}(a_3 + d_5 C_4) + a_2 C_2) \Theta'_{2(\text{slave})} &= (C_{23}(d_6 C_4) + a'_2 C_2) \Theta'_{2(\text{master})} \end{aligned} \quad (27)$$

Therefore mapping factors are known from (27),

$$\Theta'_{4(\text{slave})} = \frac{(d_6)}{(d_5)} \Theta'_{4(\text{master})}$$

$$\Theta'_{3(\text{slave})} = \frac{(d_6 C_4)}{(a_3 + d_5 C_4)} \Theta'_{3(\text{master})} \quad (28)$$

$$\Theta'_{2(\text{slave})} = \frac{(C_{23}(d_6 C_4) + a'_2 C_2)}{(C_{23}(a_3 + d_5 C_4) + a_2 C_2)} \Theta'_{2(\text{master})}$$

Where,

$$a_2=50 \text{ mm}, a_3=15 \text{ mm}, d_5=30 \text{ mm}, a'_2=138 \text{ mm}, d_6=60 \text{ mm}$$

All mapping factors are defined on table 5 to meet  $\Theta'_{\text{slave}} = (\text{mapping factor})\Theta'_{\text{master}}$ .

**Table 6.** Mapping factors between master and slave

Joint i	mapping factors
1	On / Off switch
2	$\frac{(C_{23}(d_6 C_4) + a'_2 C_2)}{(C_{23}(a_3 + d_5 C_4) + a_2 C_2)}$
3	$\frac{(d_6 C_4)}{(a_3 + d_5 C_4)}$
4	$\frac{(d_6)}{(d_5)}$
5	1
6	1

Although  $v_y$  and  $v_z$  are exactly same between master device and slave robot through the mapping factors,  $v_x$  has an error. From (25), (26), and (28) the error is

$$(S_{23}(d_6C_4) + a'_2S_2) - \frac{(C_{23}(d_6C_4) + a'_2C_2)}{(C_{23}(a_3 + d_5C_4) + a_2C_2)} \times (S_{23}(a_3 + d_5C_4) + a_2S_2) \quad (29)$$

Only if  $\Theta_3$  is  $0^\circ$ , the error becomes zero. Otherwise, the error is generated as (29).

## IV. EXPERIMENTS AND RESULTS

### 4.1 Measuring velocity and results

In this experiment, we investigate whether the tip of the slave robot for rotational joints has similar velocity master device using mapping factors developed in the previous section. First, reconstructed master device and slave robot were depicted by using MATLAB. Then, we measure the trajectories of the master device and slave robot, applying mapping factors to each joint of slave robot from table 6. In case of two prismatic joints, joint 1 is controlled by on/off switch and joint 5 is manipulated by 1:1 mapping. In case of four rotational joints, the mapping factor of joint 2 is  $\frac{(c_{23}(d_6c_4) + a_2c_2)}{(c_{23}(a_3+d_5c_4) + a_2c_2)}$ . When the master device was rotated from 0 to 30 degrees, the slave robot should be rotated from 0 to 62.5 degrees to have similar velocity of both tips. As a result, both tips moved 103.6 mm at the same time as shown in figure 20. For joint 3, the mapping factor is  $\frac{(d_6c_4)}{(a_3+d_5c_4)}$ . Therefore, if the master device was rotated from 0 to 30 degrees, the slave robot should be rotated from 0 to about 40 degrees. Also, we can find that they moved same distance 31.4 mm at the same time as shown in figure 21. In case of joint 4, the factor is  $\frac{(d_6)}{(d_5)}$ . When the master device was rotated from 0 to 30 degrees, we make the slave robot move from 0 to 60 degrees. Then, they have same distance 31.4 mm at the same time as shown in figure 22.

From this experiments, when a joint is rotated and the other joints are zero, the trajectory error of

both tips could be zero by using mapping factors.

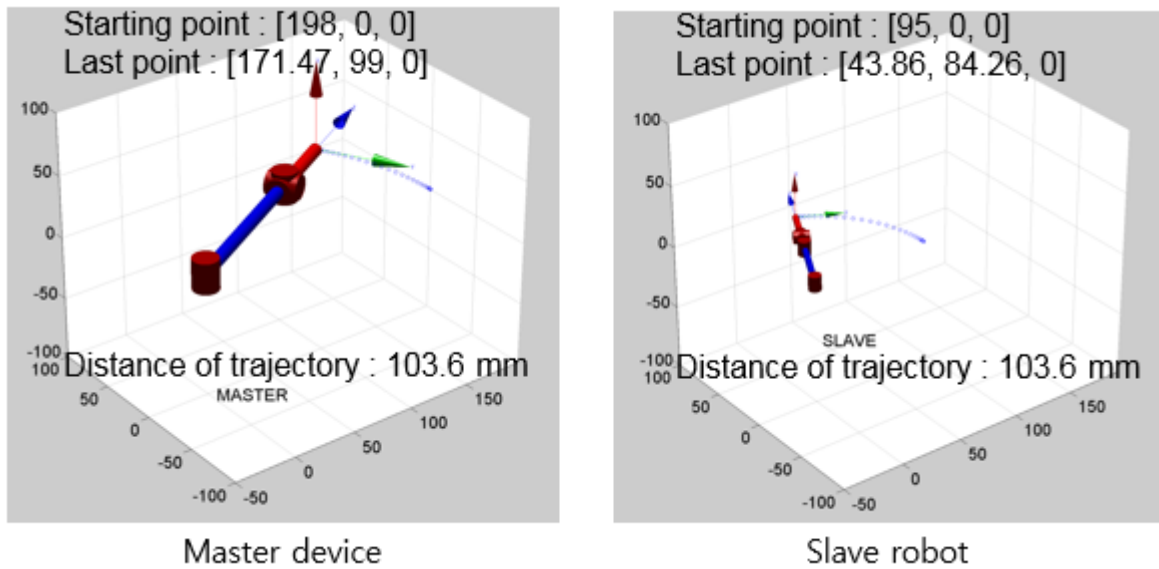


**Fig. 20** Comparison of the trajectories between master and slave about joint 2

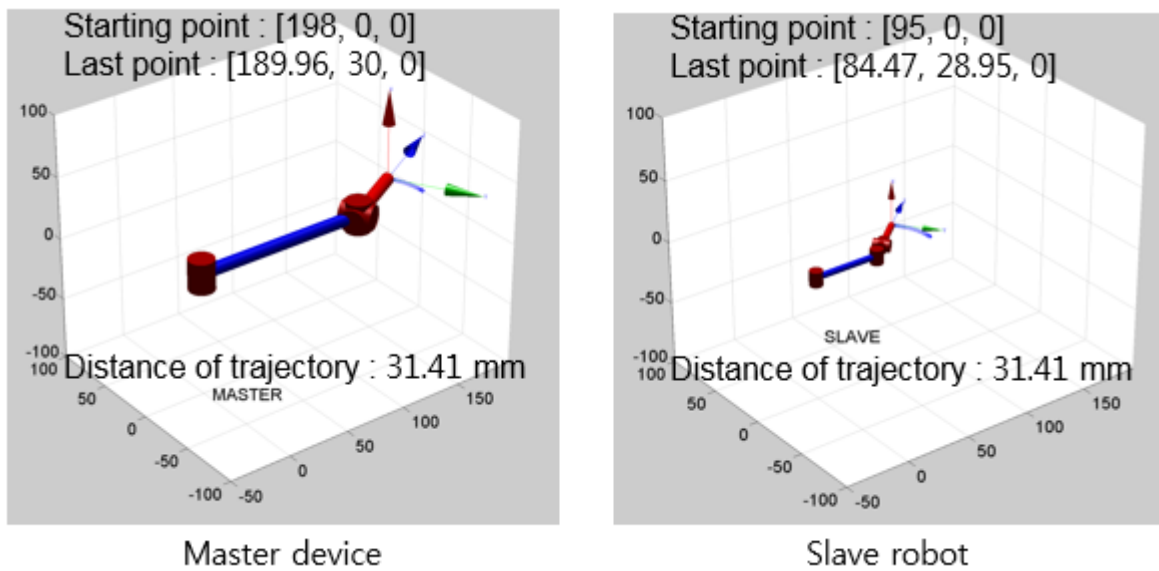


**Fig. 21** Comparison of the trajectories between master and slave about joint 3

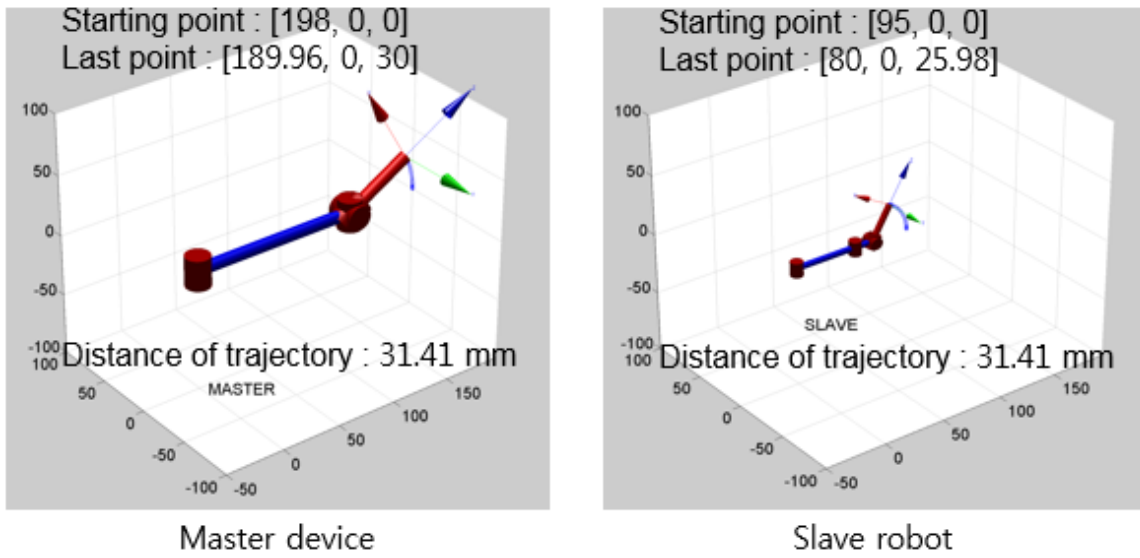


**Fig. 22** Comparison of the trajectories between master and slave about joint 4

However, when joint 2 is rotated and joint 3 is not  $0^\circ$ , the trajectories between them have error like (29). The figure 23 and 24 show the error of them according to different angle of joint 3. When the angles of joint 3 are  $30^\circ$  and  $60^\circ$ , errors are generated as 8.5 mm and 4.46 mm respectively.

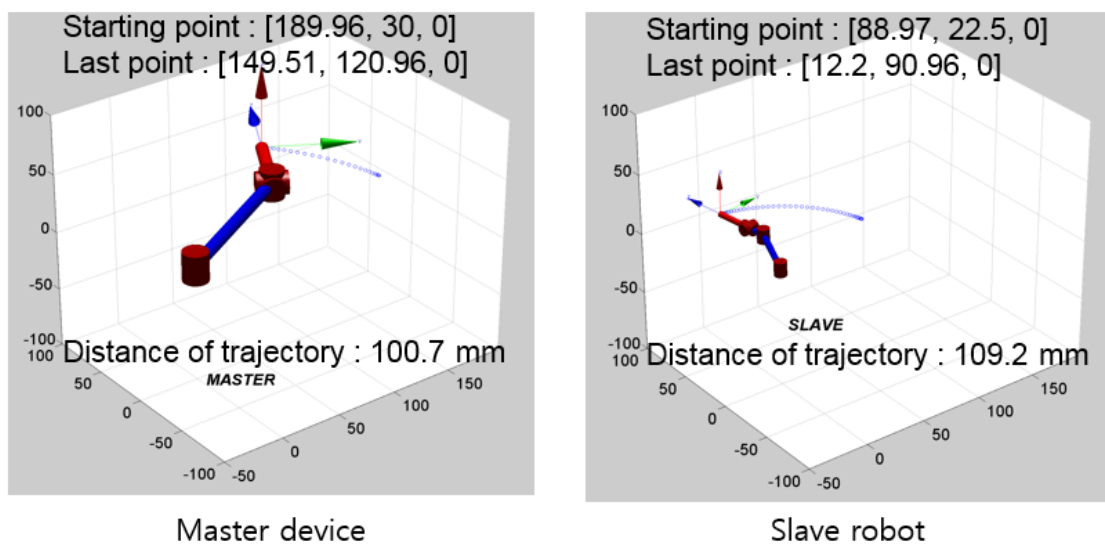


**Fig. 23** Comparison of the trajectories between master and slave about joint 2 ( $\Theta_3 = 30^\circ$ )

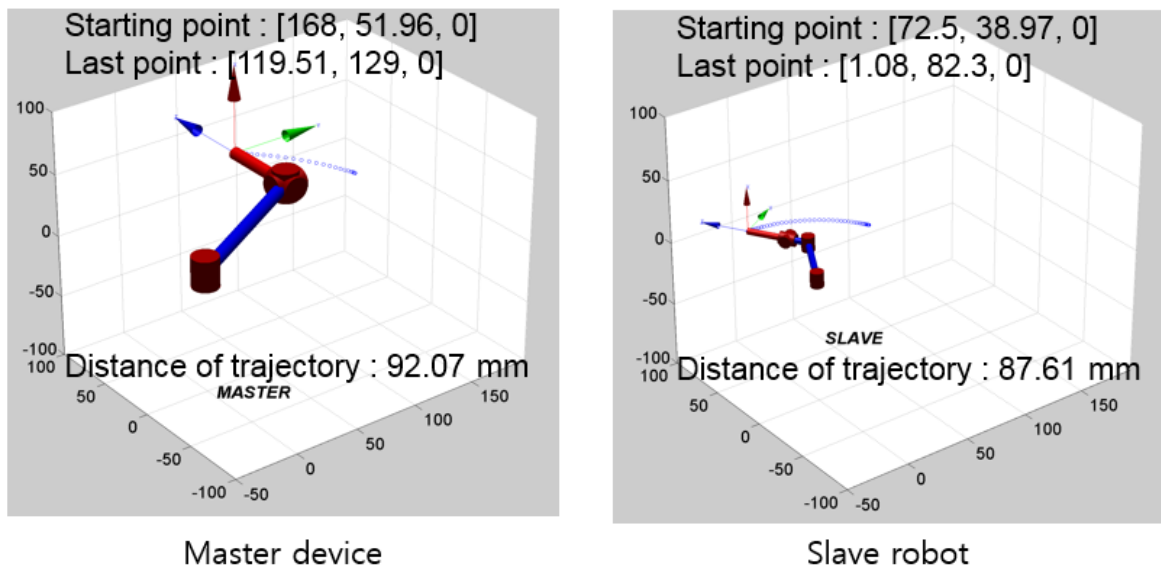


**Fig. 24** Comparison of the trajectories between master and slave about joint 2 ( $\Theta_3 = 60^\circ$ )

## 4.2 Simulation with virtual slave robot and results

For measuring the velocities of the tips between the master device and slave robot in real time, we made simulation by using VTK based on Open GL. The simulation system consists of real master device, ARDUINO, and virtual master slave in PC as an input device, an electronics prototyping platform, and a display showing the output respectively as shown in figure 25. When the encoder values are obtained from real master device, ARDUINO translates the encoder pulses into joint angles of the virtual master device. Then, the program multiplies the mapping factors to each joints of virtual slave robot. Finally, we can obtain the trajectories of virtual master device and slave robot by manipulating the real master device.

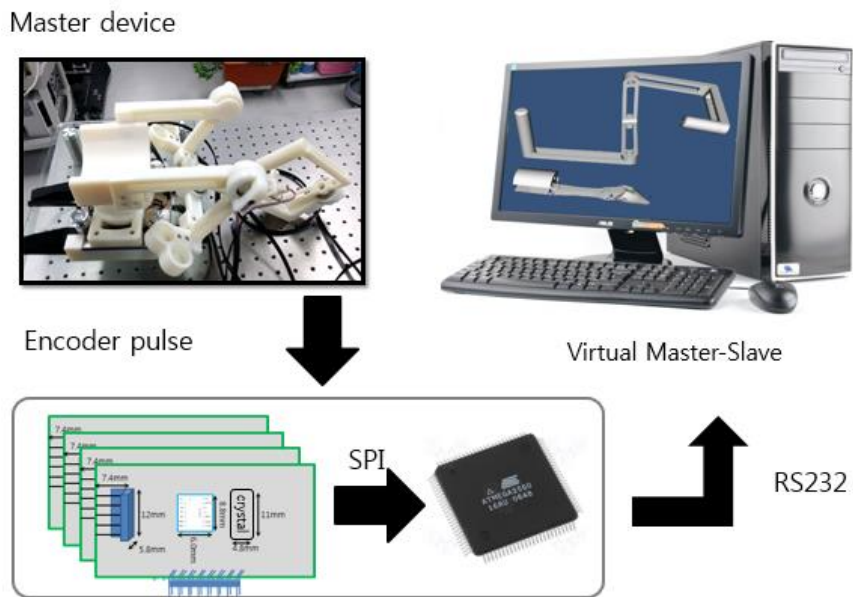


**Fig. 25** Simulation system for measuring trajectory of virtual master device and slave robot

In order to compare the trajectories of the tips between virtual master and slave, four rotational joints of the real master device was arbitrarily manipulated. Although they have error about 8 mm generated from (29), the shape and distance of trajectory are almost same as shown in figure 26.

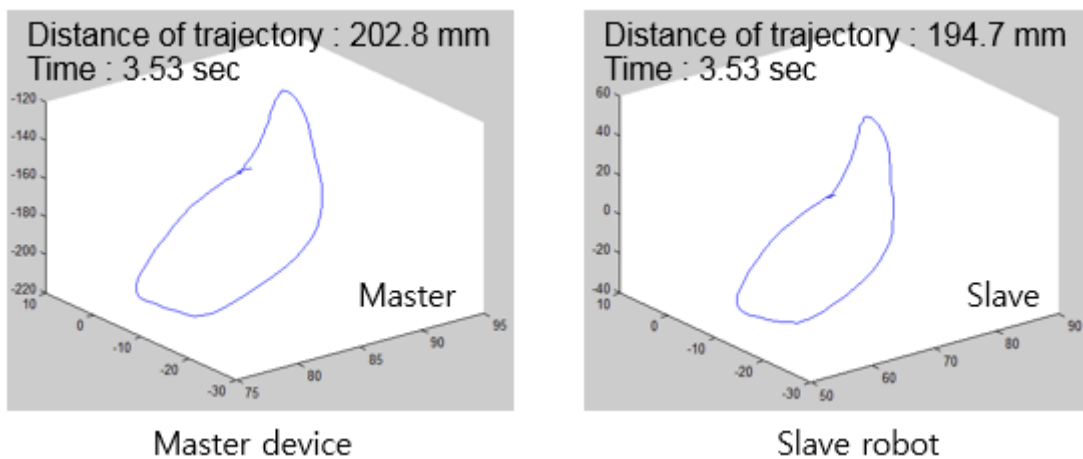


**Fig. 26** Comparison of trajectories between virtual master and slave for four rotational joints

## V. CONCLUSION AND DISCUSSION

In this paper, an ergonomic master device has been developed to control all joints of Y-type SPLS robot. Based on deep understanding of the SPLS and Y-type SPLS robot, the goal of this paper is to develop a suitable master device for Y-type SPLS robot. In order to achieve this goal, the target robot PLAS was analyzed in detail. Since all joints of the robot are inserted in the human body during the surgery, all joints controlling method is adopted for increasing the surgical safety. The two main factors of the research are development of an ergonomic master device and evaluation of mapping factors to decouple each joint.

First, we developed an ergonomic master device to reduce the surgeon's fatigue, considering that SPLS requires high concentration and long operation time. When we apply all joints controlling method to the master device, each joint of slave robot should be corresponded to each joint of human arm. If only structure of slave robot is considered, it might occur limited motion to manipulate the master device and lead to fatigue for operators. In order to minimize amount of metabolism for manipulating the master device, three rotational joints are placed at wrist joint. Beside, for decoupling two prismatic joints of slave robot, the master device was designed to make the joints be manipulated by translation of shoulder and fingers.

Finally, the 6 DOF master device was developed, adding the rotational joint at the elbow joint for triangulation. Also, the counterbalancing was applied for the positioning stage and less inertia.

Secondly, since master device has different structure from the slave robot for ergonomic design, the velocities of tips between master device and slave robot are different by using simple 1 by 1 matching. Although inverse kinematics generally can be used to have same velocity of both tips, some joints might be coupled and all joints controlling method can not be realized. Since an error of velocities between them is unavoidable for all joints controlling method, we try to minimize the error through the special mapping factors. A suitable mapping factors was calculated from both velocity and implemented in the simulation. Using the mapping factors, we can get same  $v_y$  and  $v_z$  of both tips except for  $v_x$ . We verified that the shape and distance of trajectory are almost same through the simulation.

In this study, when the length of each joint was determined, the average length of human arm was considered. However, the average value could not make all operators be satisfied. In order to make all operators be satisfied, the master device will be designed to be tailored to the each length of the human arm. Also, we will introduce haptics into our master device to provide force feedback for operators. It will ensure a more precise and safer surgery. Finally, our master slave system has the velocity errors of both tips. We have

to effort to reduce or remove the error through the approach of a new mechanism and control method.

If these problems could be solved, the designed master device would be expected to be used as widely for all Y-type SPLS robots.

## References

- [1] R. Veldkamp, E. Kuhry, W. C. Hop, J. Jeekel, G. Kazemier, H. J. Bonjer, E. Haglind, L. Pählman, M. A. Cuesta, S. Msika, M. Morino, A. M. Lacy. (2005) Jul. "Laparoscopic surgery versus open surgery for colon cancer: short-term outcomes of a randomised trial," *The Lancet Oncology*, 6 (7) pp. 477-84.
- [2] R. S. Chamberlain, S. V. Sakpal. (2009) Sep. "A Comprehensive Review of Single-Incision Laparoscopic Surgery (SPLS) and Natural Orifice Transluminal Endoscopic Surgery (NOTES) Techniques for Cholecystectomy," *Journal of Gastrointestinal Surgery*, 13 (9) pp. 1733-1740.
- [3] R. Autorino, R. J. Stein, E. Lima, et al. (2010) May. "Current status and future perspectives in laparoendoscopic single-site and natural orifice transluminal endoscopic urological surgery," *International Journal of Urology*, 17 (5) pp. 410-431.
- [4] J. H. Kaouk and R. K. Goel. (2009) May. "Single-port laparoscopic and robotic partial nephrectomy," *European Urology*, 55 (5) pp. 1163-1169.
- [5] M. T. Gettman, W. M. White, M. Aron, et al. (2011) Feb. "Where do we really stand with LESS and NOTES?," *European Urology*, 59 (2) pp. 231-234.
- [6] J. H. Kaouk, G. P. Haber, R. K. Goel, M. M. Desai, M. Aron, R. R. Rackley, C. Moore and I. S. Gill. (2008) Jan. "Single-Port Laparoscopic Surgery in Urology: Initial Experience," *Urology*, 71 (1) pp. 3-6.
- [7] J. D. Raman, A. Bagrodia, J. A. Cadeddu. (2008) Feb. "Single-Incision, Umbilical Laparoscopic versus Conventional Laparoscopic Nephrectomy: A Comparison of Perioperative Outcomes and Short-Term Measures of Convalescence," *European Urology*, 55 pp. 1198-1206.

- [8] J. H. Kaouk, R. K. Goel, G. P. Haber, S. Crouzet and R. J. Stein. (2009) Feb "Robotic single-port transumbilical surgery in humans: initial report," *British Journal of Urology International*, 103 (3) pp. 366-369.
- [9] R. Autorino, J. A. Cadeddu, M. M. Desai, et al. (2011) "Laparoendoscopic single site and natural orifice transluminal endoscopic surgery in urology: a critical analysis of the literature," *European Urology*, (59) pp. 26-45.
- [10] L. Cindolo, S. Gidaro, F. R. Tamburro and L. Schips. (2010) May. "Laparo-endoscopic single-site left transperitoneal adrenalectomy," *European Urology*, 57 (5) pp. 911-914.
- [11] A. R. Lanfranco, A. E. Castellanos, J. P. Desai and W. C. Meyers. (2004) Jan. "Robotic Surgery: A Current Perspective," *Annals of Surgery*, 239 (1) pp. 14-21.
- [12] G. Haber, M. A. White, R. Autorino, et al. (2010) Dec "Novel Robotic da Vinci Instruments for Laparoendoscopic Single-site Surgery," *Urology*, 76 (6) pp. 1279-1282.
- [13] R. Autorino, J. H. Kaouk, J. U. Stolzenburg, et al. (2012) Aug. "Current Status and Future Directions of Robotic Single-Site Surgery: A Systematic Review," *European Urology*, 63 pp. 266-280.
- [14] K. Xu, R. E. Goldman, J. Ding, P. K. Allen, D. L. Fowler and N. Simaan. (2009) Oct. "System design of an Insertable Robotic Effector Platform for Single Port Access (SPA) Surgery," *Intelligent Robots and Systems, IEEE/RSJ International Conference*, pp. 5546-5552.

- [15] M. Piccigallo, U. Scarfogliero, C. Quaglia, G. Petroni, P. Valdastri, A. Menciassi, and P. Dario. (2010) "Design of a Novel Bimanual Robotic System for Single-Port Laparoscopy," *IEEE/ASME Transactions on Mechatronics*, 15
- [16] B. Cheon, E. Gezgin, D. Ji, M. Tomikawa, M. Hashizume, H. Kim, J. Hong. (2014) May. "A single port laparoscopic surgery robot with high force transmission and a large workspace," *Surgical Endoscopy*, 28 (9) pp. 2719-2729.
- [17] A. J. Silva, O. A. D. Ramirez, V. P. Vega, J. P. O. Oliver. (2009) Sept. "Phantom omni haptic device: Kinematic and manipulability," *Electronics, Robotics and Automotive Mechanics Conference*, pp. 193-198.
- [18] R. Tadakuma, Y. Asahara, H. Kajimoto, N. Kawakami, and S. Tachi. (2005) Nov/Dec. "Development of anthropomorphic multi-DOF master-slave arm for mutual teleexistence," *IEEE Transactions on Visualization and Computer Graphics*, 11 (6) pp. 626-631.
- [19] K. Ikuta, T. Hasegawa, and S. Daifu. (2003) sept. "Hyper redundant miniature manipulator "hyper finger" for remote minimally invasive surgery in deep area," *IEEE International Conference on Robotics and Automation*, p. 1098-1102.
- [20] Z. M. Thant, S. C. Low, S. W. Tang, L. Phee, K. Y. Ho, S. C. Chung. (2006) "Ergonomic master controller for flexible endoscopic gastrointestinal robot manipulator," *International Conference on Biomedical and Pharmaceutical Engineering*, pp. 575-579.
- [21] J. M. Jeong, Y. S. Yoon. (2010) Jun. "Ergonomic Design of NOTES Robot System Master", *M.D. Thesis*, Korea Advanced Institute of Science and Technology, Daejeon, Republic of Korea, 52 pages.

- [22] V. Hayward, P. Gregorio, O. Greenish, M. Doyon. (1997) Jun. "Freedom-7: A High Fidelity Seven With Application To Surgical Training", *Lecture Notes in Control and Information Science* 232, pp. 445-456.
- [23] X. Wang. (1999) Jan. "A behavior-based inverse kinematics algorithm to predict arm prehension postures for computer-aided ergonomic evaluation," *Journal of Biomechanics*, 32 pp. 453-460.
- [24] S. Shim, D. Ji, J. Arata, M. Hashizume, J. Hong. (2014) Jun. "A Master Slave Y-type Single Port Laparoscopic Surgery Robot with High Force Transmission and Large Workspace," *Hamlyn Symposium on Medical Robotics*, pp. 27-28.

## 요 약 문

### Y 형태의 단일 공 복강경 수술 로봇을 위한 모든 관절을 조정할 수 있는 마스터

본 연구에서는 Y 형태의 단일 공 복강경 수술(single port laparoscopic surgery) 로봇을 위한 마스터를 개발하였다. 최근, 단 하나의 상처만을 남기는 복강경 수술의 수요가 증가함에 따라, 수술의 난이도를 낮춰주고 더욱 정밀하게 해주는 여러 수술 로봇들이 개발되고 있다. 이 수술 로봇들은 형태에 따라 X 형태와 Y 형태 로봇으로 나뉘는데, 각 문자의 교차점이 로봇이 몸으로 들어가는 상처 부분 즉 배꼽이다. X 형태의 로봇은 대부분의 관절이 몸 밖에서 움직이지만, Y 형태의 로봇은 수술 중에 모든 관절이 환자의 몸 안으로 들어가 움직이게 된다. 로봇의 끝 단만을 조정할 수 있는 일반적인 마스터를 Y 형태의 로봇에 사용 할 경우, 끝 단을 제외한 관절들이 의사의 의도에 상관없이 움직여 수술 중 환자의 장기에 피해를 줄 수 있다. 이러한 문제를 해결하고 Y 형태의 로봇 수술의 안정성을 높이기 위해 모든 관절을 조정할 수 있는 마스터를 개발하였다. 모든 관절을 조정하는 마스터 개발에서 중요한 것은 조정하는 의사의 편의성을 위한 인체공학적 설계와 섬세한 수술을 위한 마스터와 로봇 끝 단의 속도 오차를 최소화 할 수 방법을 고안하는 것이다. 우선, 고도의 집중력과 긴 수술시간을 고려하여 사람 팔의 관절을 토대로 로봇 팔의 관절에 대응시켜 인체공학적 마스터를 설계하였다. 하지만, 마스터와 로봇의 관절구조가 달라지면서 단순한 관절 간 조정으로는 마스터와 로봇 끝 단의 속도 오차가 매우 크게 된다. 이러한 오차를 최소화 하기 위해, 마스터와 로봇의 각 관절간 대응 값(mapping factor)을 구하였다. 이에, 모든 관절을 조정 가능한 마스터를 인체 공학적으로 설계, 제작한 후 마스터와 로봇간의 대응 값을 적용시킨 시뮬레이션을 통해 성능평가를 실시했다.